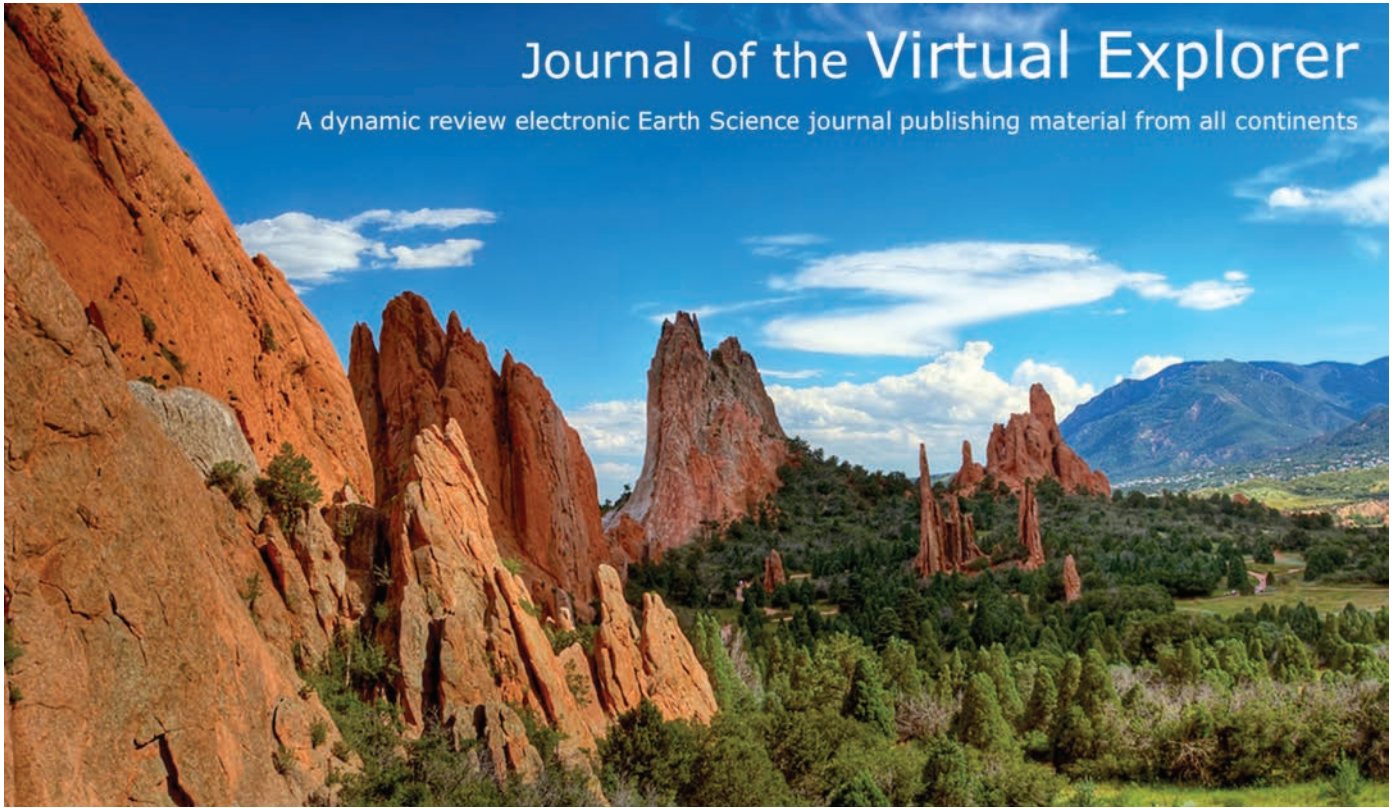


Journal of the Virtual Explorer

A dynamic review electronic Earth Science journal publishing material from all continents



Finding the Lesser Himalayan Duplex in the Himalayan Thrust Belt of Far Western Nepal amidst Forests, Villages, Farming and Leeches

Robinson D. and DeCelles P.

Journal of the VIRTUAL EXPLORER, Electronic Edition, ISSN 1441-8142, volume 47, Paper 2, DOI: 10.3809/jvirtex.2014.00341, In: (Eds) Chiara Montomoli, Rodolfo Carosi, Rick Law, Sandeep Singh, and Santa Man Rai, Geological field trips in the Himalaya, Karakoram and Tibet, 2014

Download from: <http://www.virtualexplorer.com.au/article/2014/341/finding-the-lesser-himalayan-duplex/index.html>

Click <http://virtualexplorer.com.au/subscribe/> to subscribe to the Virtual Explorer
Email team@virtualexplorer.com.au to contact a member of the Virtual Explorer team

Copyright is shared by The Virtual Explorer Pty Ltd with authors of individual contributions. Individual authors may use a single figure and/or a table and/or a brief paragraph or two of text in a subsequent work, provided this work is of a scientific nature, and intended for use in a learned journal, book or other peer reviewed publication. Copies of this article may be made in unlimited numbers for use in a classroom, to further education and science. The Virtual Explorer Pty Ltd is a scientific publisher and intends that appropriate professional standards be met in any of its publications.

Finding the Lesser Himalayan Duplex in the Himalayan Thrust Belt of Far Western Nepal amidst Forests, Villages, Farming and Leeches

Robinson D.¹ and DeCelles P.²

¹ Department of Geological Sciences, University of Alabama, Tuscaloosa AL 35487 USA.

² Department of Geosciences, University of Arizona, Tucson AZ 85721 USA.

GUIDE INFO

Keywords

Lesser Himalaya, thrust duplexes

Citation

Robinson, D. and DeCelles, P. 2014. Finding the Lesser Himalayan Duplex in the Himalayan Thrust Belt of Far Western Nepal amidst Forests, Villages, Farming and Leeches. In: (Eds.) Chiara Montomoli, Rodolfo Carosi, Rick Law, Sandeep Singh, and Santa Man Rai, Geological field trips in the Himalaya, Karakoram and Tibet, Journal of the Virtual Explorer, Electronic Edition, ISSN 1441-8142, volume 47, paper 2, DOI: 10.3809/jvirtex.2014.00341.

Correspondence to:

dmr@ua.edu
decelles@email.arizona.edu

IN THIS GUIDE

Much of the evidence for the Miocene to Pliocene evolution of the Himalayan thrust belt resides in the Lesser Himalayan rocks along the Himalayan arc. These rocks are thrust one top of one another in imbricated thrust sheets called the Lesser Himalayan duplex. The rocks and the structures crop out poorly south of the high peaks of the Himalaya; thus, the timing and sequence of thrusting in the Lesser Himalayan rocks are difficult to unravel. The field evidence, both stratigraphic and structural, dictates the location and composition of the thrust sheets; however, thermochronology and modeling aids in determining the evolution. This virtual field trip documents important locations in remote far western Nepal that help to understand and unraveling the geologic history in the Lesser Himalayan rocks.

INTRODUCTION

The southern half of the Himalayan thrust belt is composed of low-grade metasedimentary and sedimentary rocks that are collectively referred to as the Lesser Himalayan sequence. Although the low elevation and relatively humid climate in the Lesser Himalaya combine to limit outcrop exposures (relative to those of the high elevation Greater Himalaya), careful mapping accompanied by geochronology and isotope geochemistry allow the recognition of regional stratigraphy and structural geology. Thermochronology, in the context of regional balanced structural cross-sections, helps to establish the kinematic history and tectonic evolution of the thrust belt.

A geologic map of far-western Nepal was first compiled at a scale of 1:250,000 by Shrestha et al. (1987a, 1987b), illustrating the major stratigraphic packages and fault zones. Upreti (1996, 1999) compiled the work of previous researchers in central and western Nepal and showed the correlation of stratigraphy between the two regions. The work of DeCelles et al. (1998a, 2001) and Robinson et

al. (2001, 2003) provided additional stratigraphic and structural data for the large-scale study presented in Robinson et al. (2006) that includes a map and three cross-sections. Pearson & DeCelles (2005) documented the stratigraphic and structural context of the Ramgarh thrust (Fig. 1), which was then extended across the whole Himalayan arc in Robinson & Pearson (2013) and referred to as the Ramgarh-Munsiari thrust. The three cross-sections were forward modeled in Robinson (2008), providing a clear picture of the structural evolution of the Himalayan thrust belt. DeCelles et al. (2001) and Robinson et al. (2001, 2006) used a combination of cross-cutting relationships and the detrital unroofing record of Miocene-Pliocene foreland basin deposits to develop a kinematic history in far-western Nepal. However, thermochronologic data needed to assess the history of rock exhumation in far-western Nepal are still sorely lacking (e.g., Robinson et al., 2006). Bollinger et al. (2004) provided important thermal constraints on Lesser Himalayan rocks using Raman spectroscopy of carbonaceous minerals (RSCM) data. The foreland basin de-

posits in front of the Himalayan thrust belt were dated using magnetostratigraphy (Appel & Rösler, 1994; Rösler et al., 1997; Gautam & Rösler, 1999; Gautam et al., 2000; Ojha et al., 2000, 2009) and a temporally constrained shift in the carbon isotope composition of organic matter (Ojha et al., 2000, 2009) and tied to periods of time when the thrust belt was deforming and eroding (e.g., DeCelles et al., 2001; Huyghe et al., 2001; Mugnier et al., 2004; Najman et al., 2004, 2009; van der Beek et al., 2006; Szulc et al., 2006; Ravikant et al., 2011). Robinson & McQuarrie (2012) used forward modeling reconstructions and these data in the thrust belt and foreland basin to tie the erosional unroofing and associated deposition to the kinematics and age of fault motion. Thus, western Nepal provides a testing ground in the Himalaya for assessing structural models and the evolution of the thrust belt.

The purpose of this paper is to provide a unifying view of the Himalayan thrust belt in far-western Nepal (Fig. 1) via a virtual field trip that highlights key regions for stratigraphic and structural insights. Figure 2 is a generalized version of the geologic map from Robinson et al. (2006) and marks key locations detailed in this manuscript. Figure 3 shows two cross-sections that illustrate the structural geology. Remote far-western Nepal does not have a well-developed hostelry infrastructure. Thus, the first half of this field trip may be accessed by road with camping but the second half can only be accessed by hiking and camping. On May 2, 2000, GPS errors instantaneously changed from 100 m to 10 m; thus, some of the GPS locations acquired before this change may have errors of up to 150 m.

DAY 1. Travel from Kathmandu to Nepalgunj

Under ideal circumstances, travel from Kathmandu to far-western Nepal takes two-three days along the Mahendra Highway; alternatively, daily flights depart Kathmandu for Nepalgunj. The advantage of flying is that, on clear days, spectacular views of the High Himalaya are available out the starboard windows of the aircraft. Spend the night at a hotel in Nepalgunj or Dhangarhi (Camp 1 on Fig. 2).

DAY 2. Travel north from Nepalgunj to Budar.

Today we begin the excursion into the Himalayan thrust belt by vehicle. Driving to Budar without observing the geology would be a 3 hour trip; however, the trip to Budar will take all day with stops.

Subhimalayan thrust system

The Subhimalayan (SH) zone is the frontal 10–35-km-wide belt composed of the 4-6 km thick Miocene-Pleistocene Siwalik Group foreland basin deposits, which have been incorporated into the frontal part of the thrust belt. Three informal units are recognized -- the lower, middle, and upper members (Tokuoka et al., 1986; Harrison et al., 1993; Quade et al., 1995; DeCelles et al., 1998a). This subdivision is lithostratigraphic, and so it is useful for broad regional comparisons but cannot be used for detailed chronostratigraphy (DeCelles et al., 1998a; Ojha et al., 2009). Because continuously exposed sections of the Siwalik Group are not exposed along the main road, detailed chronostratigraphic and sedimentologic work in far-west Nepal was done along Khutia Khola (Fig. 2) a few km east of the main highway; thus, no field stops in the Siwalik Group are listed. Fine regional vistas of the Siwalik Group and the Subhimalayan thrust belt are available to the west while driving along the road toward Dadeldhura, and numerous exposures are present in roadcuts. Exercise caution when pulling over to inspect roadcuts, and avoid blind curves.

The topographic front of the SH foothills is the Main Frontal thrust (MFT); however, the thrust is not exposed at the surface (Figs. 2 and 3a). North of the MFT are the SH rocks. The Siwalik Group was shed from the rising Himalaya at Khutia Khola by ca. 13.3 Ma (Ojha et al., 2000); however, the base is covered by alluvium so the unit may be as old as 15.1 Ma, the youngest documented age of the LH Dumri Formation rock (DeCelles et al., 1998a). The entire Siwalik Group is unmetamorphosed and coarsens upward. The lower unit is composed of relatively thin sandstone channel deposits and reddish overbank siltstone and calcic paleosols (Fig. 4a). At Khutia Khola, the lower Siwalik unit is at least 862 m thick, and consists of interbedded sandstones and mudrocks (DeCelles et al., 1998a). Detrital zircon U-Pb ages show age populations of ca. 500-800 Ma; 1000-2100 Ma

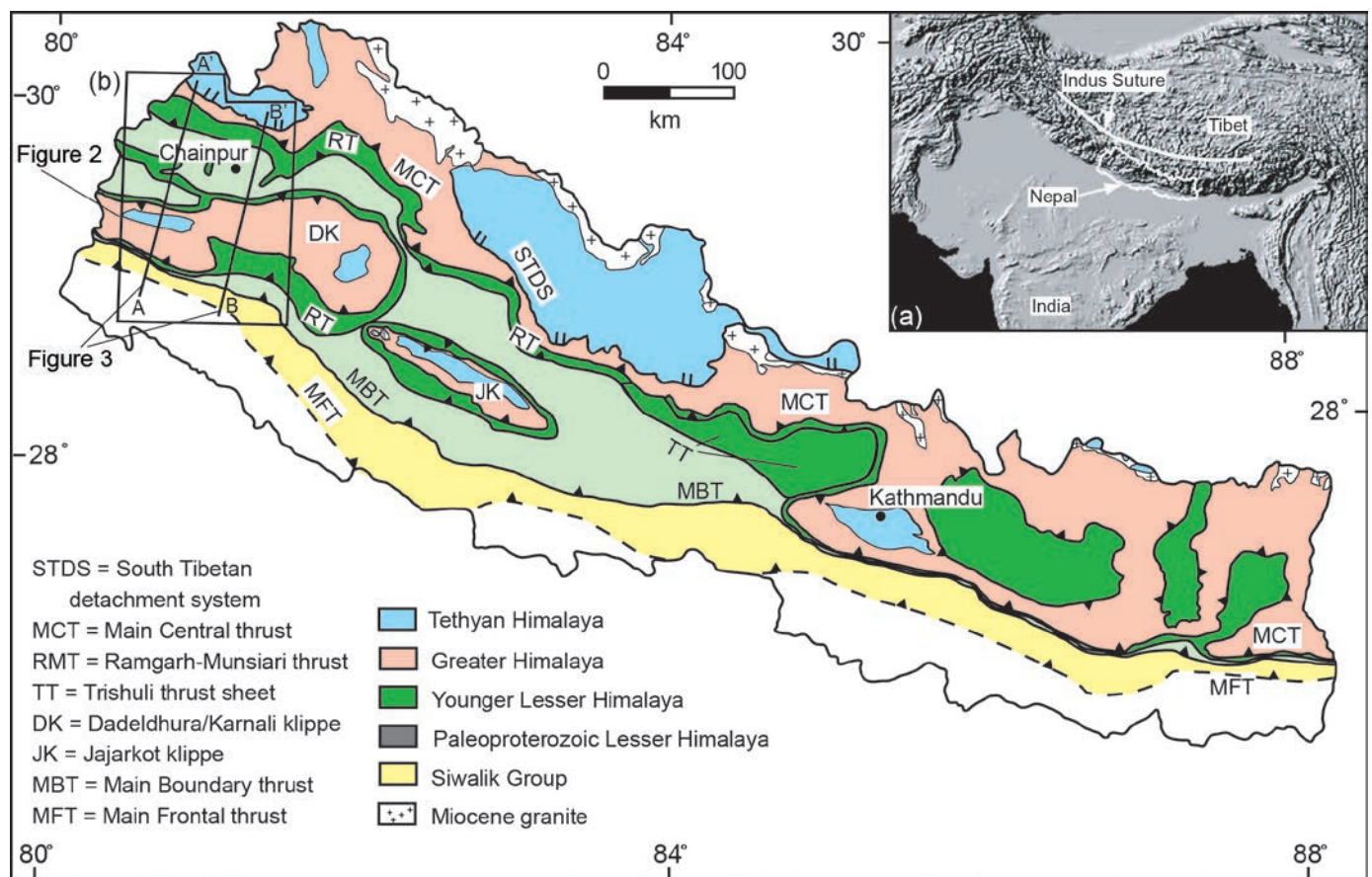


Figure 1

a) Digital Image of the Himalayan-Tibetan orogenic system from the Global 30 Arc Second Elevation Data Set. Nepal is outlined in white for reference. (b) Geologic Map of Nepal modified from Robinson & Pearson (2006) and loosely based on Amatya & Jnawal (1994). Black box outlines the geologic map in Figure 2. Cross section lines from Robinson et al. (2006) are marked by two parallel black lines and are shown in Figure 3. Thrust faults are indicated with barbs. Normal faults are indicated with two small parallel lines. Cities are indicated with a solid black circle.

and 2400-3200 Ma, with an upsection increase in grains from the 450-500 Ma and ~1000-1500 Ma populations (DeCelles et al., 2004). The first appearance of high-grade metasedimentary lithic grains, kyanite, and sillimanite, derived from rocks of Greater Himalayan (GH) affinity occurs in the upper part of the lower Siwalik unit (DeCelles et al., 1998b) dated at ca. 11 Ma (Ojha et al., 2000). The average $\epsilon\text{Nd}(\text{T})$ value is -16 (Huyghe et al., 2001; Robinson et al., 2001).

The lithologic change from lower to middle Siwalik units is at 10.8 Ma at Khutia Khola (Ojha et al., 2000). The middle Siwalik unit at Khutia Khola is 2468 m thick and is characterized by stacked multistory channel sandstones separated by thin, gray overbank mudstone beds and both calcic and histic paleosols (DeCelles et al., 1998a) (Figs. 4b and 4c). Clasts of limestone and dolostone derived from the LH Lakharpata Group first appear at the base of the middle Siwalik unit at

~10.8 Ma and their abundance increases upsection (DeCelles et al., 1998a) indicating derivation from the LH duplex. An upward excursion in the $87\text{Sr}/86\text{Sr}$ ratio of pedogenic carbonate nodules in mudstones of the Siwalik Group at ~9 Ma is another indication of LH carbonate erosion (Quade et al., 1997). In addition, $\epsilon\text{Nd}(\text{T})$ values become more negative from -16 to -18 between 10 and 9 Ma and remain at these values throughout deposition of the middle Siwalik unit (Robinson et al., 2001). Hinterland $\epsilon\text{Nd}(\text{T})$ values are presented in Table 1. Szulc et al. (2006) found similar up-section trends in $\epsilon\text{Nd}(\text{T})$ values and $87\text{Sr}/86\text{Sr}$ ratios of whole rock mudstone and conglomerate matrix samples in three sections of the Siwalik Group in western and far-western Nepal. Combined with $40\text{Ar}/39\text{Ar}$ ages from detrital white micas, these data were interpreted by Szulc et al. (2006) as evidence for the onset of significant erosion of Lesser Himalayan rocks in the Lesser Himalayan duplex

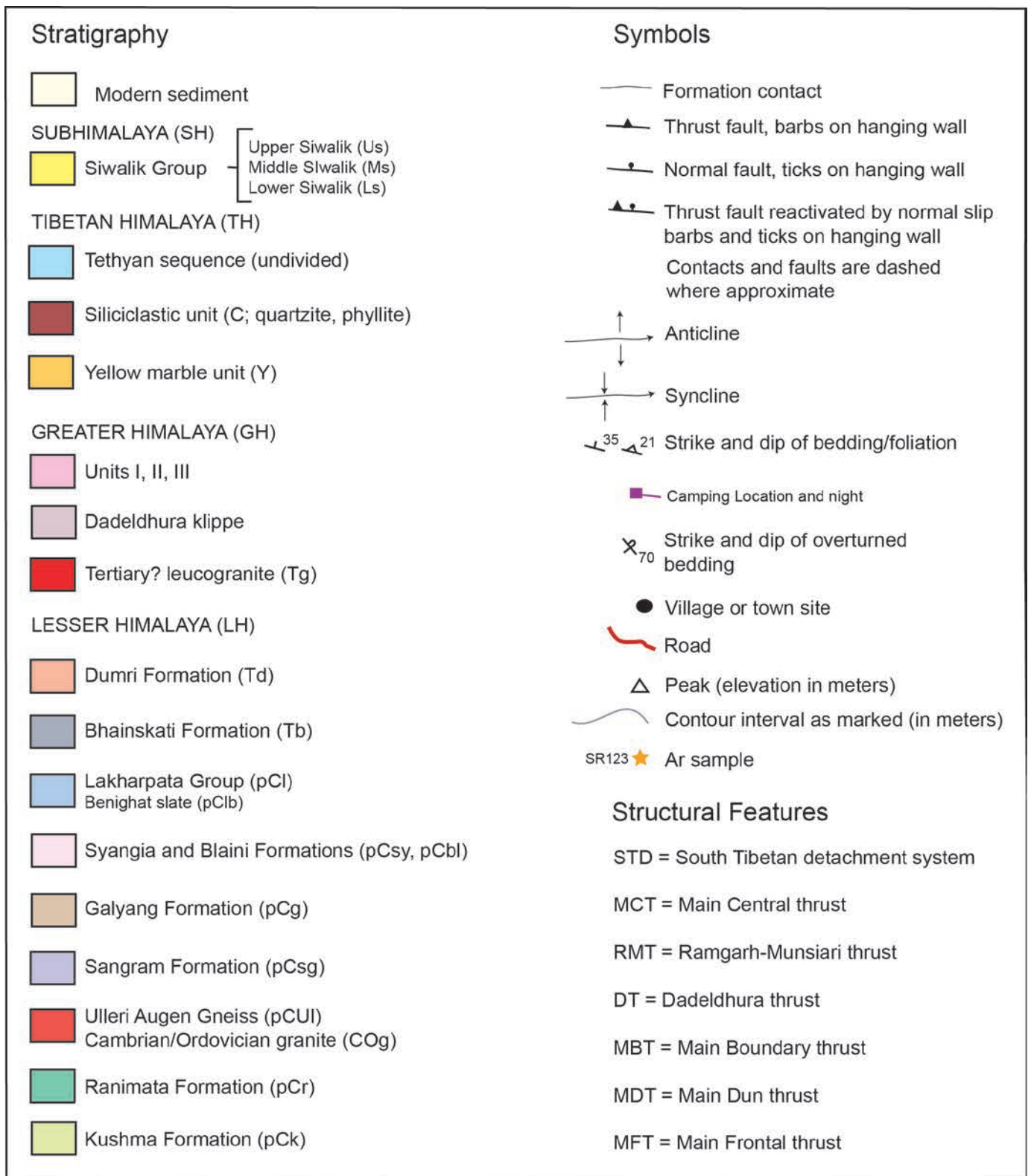


Figure 2
Western Nepal Map with camp locations and photos modified from Robinson et al. (2006).

by about 12-10 Ma.

The middle to upper Siwalik unit transition at Khutia Khola has not been dated by paleomagnetic stratigraphy (Ojha et al., 2000). At Surai Khola, this lithological transition was dated at ~3.2 Ma (Ojha et al., 2009). The upper Siwalik unit at Khutia Khola is at least 1000 m thick, and is dominated by fluvial conglomerate and sandstone, with histic paleosols (DeCelles et al., 1998a) (Fig. 4d). Detrital $\epsilon\text{Nd}(T)$ and $87\text{Sr}/86\text{Sr}$ ratios continue the upsection trends documented in the middle Siwalik unit (Szulc et al., 2006), and an increase in conglomerate clasts derived from LH rocks (quartzite and carbonate clasts) indicates emergence of local Lesser Himalayan sources in the hanging wall of the Main Boundary thrust (MBT; DeCelles et al., 1998b).

The Siwalik Group strata are imbricated on top of one another in 3 thrust sheets in the SH thrust system (Figs. 4e and 4f). The southernmost panel of lower, middle, and upper Siwalik Group rocks is carried by the MFT. The next thrust sheet to the north is the Main Dun thrust and carries only the lower and middle Siwalik Group rocks (Mugnier et al., 1999). North of that thrust sheet is third unnamed thrust sheet carrying lower and middle Siwalik Group rocks.

Lesser Himalayan Rocks South of the Dadeldhura Klippe

The MBT is the last thrust in the LH duplex system and separates LH rocks to the north from SH rocks to the south. The MBT (N29°05'13.6"; E80°34'09.4"; 1335±24 m) is not apparent along the road because it is buried by Quaternary gravel composed of quartzite clasts. Cross section A-A' (Fig. 3a) necessitates that the MBT has been reactivated as a normal fault, and may explain the modern conglomerate deposit.

The Lesser Himalaya throughout Nepal is composed of three stratigraphic successions that are separated by major regional unconformities: the Lesser Himalayan sequence; the Gondwana sequence; and the Eocene-lower Miocene foreland basin sequence (Fig. 5). The LH sequence has a thickness of ~10-13 km in central Nepal (Sakai, 1985; Upreti, 1996, 1999; Pearson, 2002). In western Nepal, the stratigraphic thickness may be similar, but structural complexity hampers an accurate estimate. In far western Nepal, Robinson et al. (2006) use an estimated thickness of 8.7-10.9 km of the LH rocks to balance the cross sections as es-

timated from map thicknesses and the thicknesses determined in the cross section.

Spend the night camping at Budar (Camp 2 on Fig. 2).

DAY 3. Lesser Himalayan Imbricate Zone, Ramgarh-Munsiari Thrust Sheet, Dadeldhura Klippe

Sangram Formation

The Sangram Formation as mapped by Shrestha et al. (1987a) in far-western Nepal is ~500 m thick and consists of a lower quartzite interval and an upper fine-grained interval, although this unit may be the Kushma Formation. The quartzite is locally referred to as the Budar quartzite, and is a white, sugary, medium-grained, orthoquartzite. However, the detrital zircon spectra of the Budar quartzite (Gehrels et al., 2011) is similar to age spectra from quartzites in the lower part of the Lesser Himalayan sequence, particularly the Kuncha Formation in central Nepal (Martin et al., 2011). The main age peaks in the Kuncha Formation and Budar quartzite are between 1900 Ma and 1960 Ma, and the complete age spectra are nearly identical. This calls into question the correlation from Shrestha et al. (1987a) that the Budar quartzite is within the Sangram Formation. Instead, the detrital zircon spectra is more similar to the Kushma Formation, the oldest LH unit in far-western Nepal. The Budar quartzite is a ridge former, but is thinner and less well-indurated than the Kushma Formation. Overlying the Budar are black argillite, brown phyllite, and thin, white to pink quartzite with occasional pebbly layers. These units are slope-formers and generally not well exposed.

Small-scale structures in the Sangram Formation are common and include small folds and faults in thinly bedded quartzite layers. Detrital zircons extracted from the Sangram Formation are dominated by ages ~1.68 Ga, indicating that the Sangram must be younger than that age (DeCelles et al., 2000). The upper contact is gradational into the Galyang Formation. The Sangram Formation along the road is pervasively folded and faulted (Fig. 6a; N29°06'24.5"; E80°34'24"; 1535±54 m).

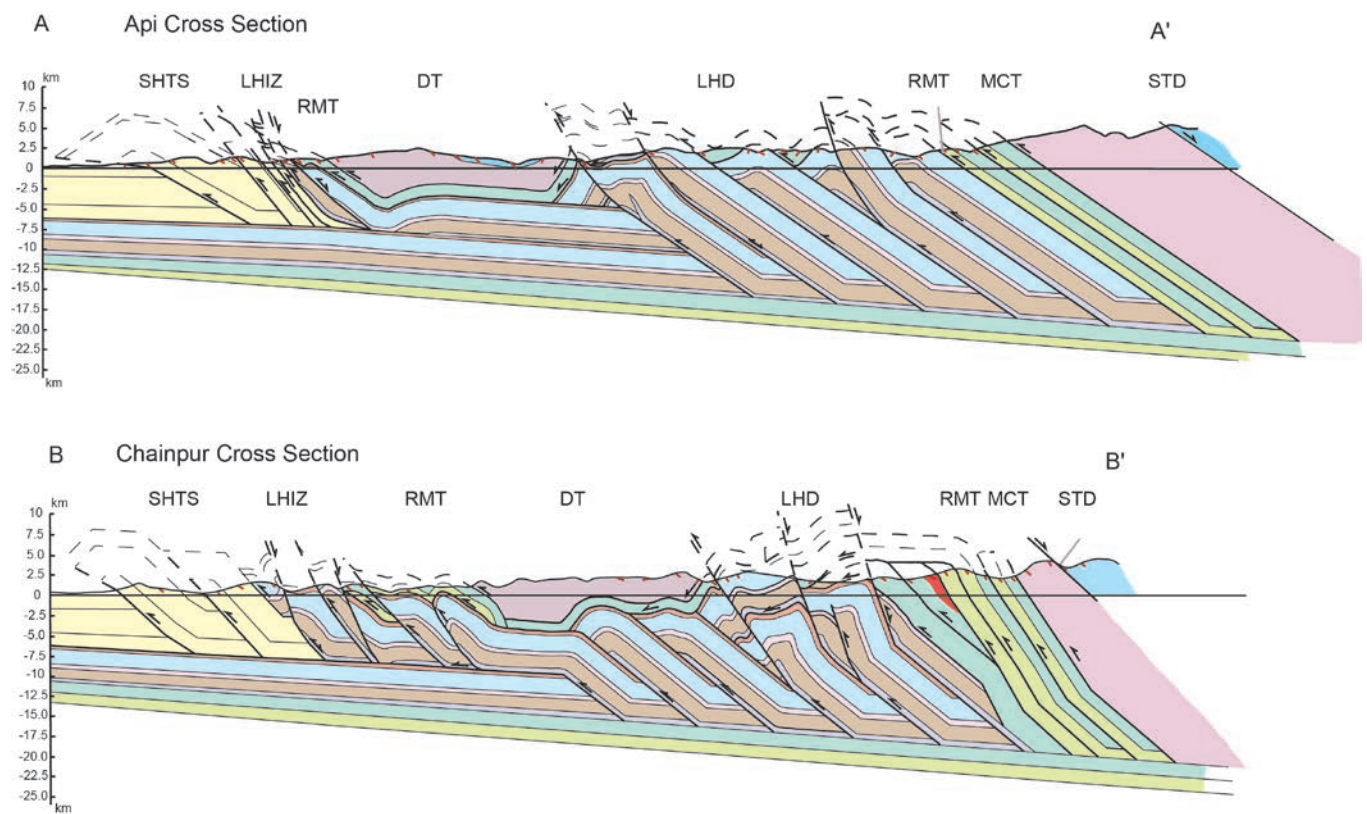


Figure 3 Geological cross-sections (a) Api and (b) Chainpur modified from Robinson et al. (2006).

Table 1 Hinterland ND data.

Thrust Sheet	Rock Type	Sample	Formation	$\epsilon Nd(0)$ value	Location
DT/MCT, TH	Shale	DD-31	Melmura	-17.6	N29°18'00.5"; E80°35'19.3"
DT/MCT, TH	Shale	DD-33	Melmura	-20.1	N29°17'44.3"; E80°38'18.4"
DT/MCT, GH	Granite	DDG-98	Cambrian-Ordovician	-11.8	n/a
DT/MCT, GH	Schist	DD-40	Kalikot	-7.6	N29°08'31.2"; E80°34'50.3"
LH duplex	Shale	SR-37	Benighat	-19.7	Seti River, north of DK
LH duplex	Shale	SR-35	Benighat	-20.7	N29°30'9.3"; E80°7'19.0"
	Shale	DD-58	Benighat	-23.6	N29°29'56.8"; E80°39'39.3"
LH duplex	Phyllite	CH-1	Galyang	-23	Near N29°35'42.4"; E81°15'5.0"
	Phyllite	DD-15	Galyang	-17.5	N29°26'43.4"; E80°37'54.7"
LH duplex	Shale	DD-52	Sangram	-15.9	N29°24'27.6"; E80°37'16.9"
LH duplex	Gneiss	SR-30	Proterozoic	-19.3	Near N29°40'15.7"; E81°20'7.2"

All Data from Robinson et al. (2006)

† n/a = not available



Figure 4

(a) Lower Siwalik Group in Khutia Khola. Photo shows a crevasse splay (below), channel (above), and red calcic paleosol deposit. Long edge of scale is 20 cm long. (b) Middle Siwalik Group showing stacked sandstone deposits. Road for scale. (c) Middle Siwalik Group in Khutia Khola. Photo shows stacked multistory sandstone channel deposits. Height of outcrop is approximately 7 m. (d) Upper Siwalik Group along the Dadeldhura road, showing a well-organized conglomerate near the village of Kanidanda. 0.3 m rock hammer for scale. (e) A rare clear view looking to the west of the Subhimalayan thrust system from the Dadeldhura road. High cliffs in the back ground are mostly in the middle Siwalik Group. (f) The Subhimalayan thrust system from the MBT looking south at sunset.

Figure 5
Lesser Himalayan stratigraphy modified from Robinson et al. (2006). Numbers in right hand column indicate approximate thicknesses of each unit in kilometers.

Tibetan Himalaya	North of STD	Dadeldhura Klippe		
	Tethyan Sequence NeoProterozoic-Cambrian Lower Ordovician	Ordovician (?)	Damgad Fm.	2.5-3.5
			Melmura Fm.	
STDS			>7.0	
Greater Himalaya	>480 Ma	Unit III	>2.6	
	<830 Ma	Unit I	6-15	
MCT/DT				
Lesser Himalaya	21-16 Ma	Dumri Fm.	1.2	
		Bhainskati Fm. (Mid to Late Eocene)	0.1	
		Gondwanan Unit (Late Eocene)	0.3	
		Lakharpata Group (Proterozoic)	3.0	
		Syangia Fm.	0.5	
		Galyang Fm.	0.8	
	1.68 Ga	Sangram Fm.	0.5	
	MBT			
	1.86 - 1.83 Ga	Ranimata Fm. including Ulleri augen gneiss	1.5-3.0	
	Kushma Fm.	0.8-1.5		
RMT				
Subhimalaya	>2 Ma	upper member	2.0	
		middle member	2.2	
	<14 Ma	lower member	0.8	
MFT				

Syangia Formation

Farther north along the road are roadcuts in interbedded purple quartzite and shale of the Syangia Formation. The Syangia Formation in far-western Nepal contains a wide variety of lithologies including: green phyllite; reddish, purple and green slate; pink, white and maroon thinly bedded quartzite; and thinly bedded blue and white dolostone and limestone (Fig. 6b). Along the Seti River, southwest of Chainpur, black slate and stretched pebble conglomerate are present in the formation. Thickness of the Syangia Formation is ~500 m in far-western Nepal. DeCelles et al. (2001) reported that the Syangia Formation was deposited after 1680 Ma; however, Gehrels et al. (2011) re-analysed the sample and it yielded a maximum depositional age of 1825 Ma. The upper contact of the Syangia Formation is transitional with the overlying Lakharpata Group. The cross-section (Fig. 3a) shows a thrust fault that has been reactivated as a normal fault between the Sangram and Syangia Formations.

The Ramgarh-Munsiari Thrust Sheet South of the Dadeldhura Klippe

The Ramgarh-Munsiari thrust (RMT) in different parts of Nepal carries the lowermost LH Paleoproterozoic rocks (Robinson and Pearson, 2013). The RMT sheet is folded in a syncline underneath the Dadeldhura klippe. Exposures along the road are mainly from the Ranimata Formation but there are some quartzite beds within the units and some augen gneiss exposures. However, we defer description of the Kushma Formation and the Proterozoic augen gneiss until the units are encountered south of the Main Central thrust.

The RMT is exposed along the road, where it juxtaposes vertical beds of the Ranimata Formation against quartzite of the Syangia Formation (Fig. 6b). Along the road, the Ranimata Formation is mixed with quartzite beds (Kushma Formation?) over a distance of ~5 km (Fig. 6c). The Ranimata Formation was intruded by the Gaira orthogneiss, which may be a Proterozoic augen gneiss, and some dioritic intrusions. The interbedded quartzite and phyllite with some faulting and folding are exposed at the village of Goganpani (Fig. 6c; N29°08'36.0"; E80°24'51.4"; 1762±67 m).



Figure 6

a) Fold nose in the Budar quartzite along the Dadeldhura Road. Robinson et al. (2006) interpreted this unit as the Sangram Formation. However, the detrital zircon age spectrum of this sample (Gehrels et al., 2011) is similar to the type Kuncha Formation spectrum in central Nepal (Martin et al., 2011) in all respects. The main peak in the type Kuncha Formation is at 1900 Ma and in the Budar quartzite at 1960 Ma. (b) Variegated shales, quartzite, and dolostone of the Syangia Formation are deformed in the footwall of the southern trace of the RMT along the Dadeldhura Road. (N29°06'24.5"; E80°34'24.0"; 1535±54 m). (c) Quartzite and phyllite in the immediate hangingwall of the RMT along the Dadeldhura Road (N29°08'36.0"; E80°34'51.4"; 1762±67 m). (d) The Budiganga gneiss in the north limb of the Dadeldhura klippe has an $^{40}\text{Ar}/^{39}\text{Ar}$ age of 21.1 ± 0.2 Ma (DeCelles et al., 2001). 5 cm knife for scale.

Ranimata Formation

The Ranimata Formation is a green chloritic phyllite with occasional 10-100 m thick intervals of thinly bedded white to green quartzite and rare thinly bedded carbonates (~20 m thick). Dark

green chloritic zones and quartz augen are interspersed throughout the formation. Mineralogic composition includes quartz + muscovite (sericite) + biotite + chlorite ± amphibole ± garnet ± staurolite. Small-scale structures include dissolution and crenulation cleavage and small folds.

Dioritic intrusions, including amphibolite, occur throughout the Ranimata Formation in western Nepal. Thickness of the formation ranges from 1.5 km in far-western Nepal to 2-3 km in mid-western Nepal; however, thickness and composition of the Ranimata Formation vary considerably along strike. The Ranimata Formation weathers readily to form wide valleys used for agriculture. In central Nepal, the upper contact is conformable with the Fagfog Formation (Sangram Formation equivalent; DeCelles et al., 2001). Although the upper contact has always been observed as a fault in western Nepal, the stratigraphic relationship in central Nepal and detrital zircons from the overlying Sangram Formation suggest that the Ranimata Formation may be transitional with the Sangram Formation (Martin et al., 2011).

The Dadeldhura Klippe

The Dadeldhura klippe is one of the so-called LH crystalline nappes. It is an erosional outlier of medium- to high-grade metamorphic rocks similar to GH rocks (Gansser, 1964; Stöcklin, 1980; Upreti and Le Fort, 1999). The Dadeldhura klippe contains schist, migmatitic gneiss (Fig. 6d), calcsilicate gneiss, metavolvanic rocks, orthogneiss, and granite (Fig. 7a) (Gansser, 1964; Fuchs, 1981; Arita et al., 1984; Bashyal, 1986; Upreti, 1990; DeCelles et al., 2001). The Kalikot Schist is fine- to coarse-grained with a mineral assemblage of quartz + biotite + muscovite + plagioclase feldspar + potassium feldspar + garnet ± kyanite ± tourmaline ± zircon (Fig. 7b). The Budhiganga Gneiss is a coarse-grained augen gneiss containing quartz + plagioclase feldspar + potassium feldspar + biotite + muscovite + garnet ± apatite (Fig. 6d). Similar minerals are also present in the mylonitic augen gneiss of the Salyanigad Gneiss, which may be contiguous with the Budhiganga Gneiss. The Salyanigad Gneiss yielded a concordant U-Pb zircon age of 478 ± 10 Ma (DeCelles et al., 2000). This gneiss surrounds the Dadeldhura granite, which yielded a concordant U-Pb zircon age of 492 ± 6 Ma (DeCelles et al., 1998a) and 470 ± 5.6 Ma (Einfalt et al., 1993), suggesting that the Salyanigad Gneiss is a ductilely deformed envelope around the Dadeldhura granite. The age and mineral assemblage of the granites and gneiss are similar to those of GH unit III orthogneiss. Calcsilicate rocks are also present in

the Dadeldhura klippe with a mineral assemblage of calcite + quartz + plagioclase + potassium feldspar + hornblende ± tourmaline ± epidote. The Dadeldhura klippe is ~6 km thick (DeCelles et al., 2001), although this is most likely a remnant of the original thickness of the klippe. DeCelles et al. (2001) reported an $40\text{Ar}/39\text{Ar}$ muscovite cooling age of ca. 21 Ma in the Budhiganga gneiss (sample SR40; DeCelles et al., 2001) from the northern limb of the Dadeldhura klippe. Robinson et al. (2006) reported an $40\text{Ar}/39\text{Ar}$ muscovite cooling age of ca. 25 Ma in the hanging wall of the MCT sheet (sample SR124).

An option that adds 4-5 hours to travel time in the Dadeldhura klippe is to travel to the east along the Dipayal Road to see Tibetan Himalayan (TH) rocks. Paleozoic sedimentary rocks related to the Tethyan sequence unconformably overlie metamorphic rocks in the Dadeldhura klippe (Fig. 2). The Melmura Formation, regarded by Shrestha et al. (1987a) as a Tethyan unit, consists of thinly bedded brown phyllite, brown and white intercalated quartzite, and graphitic slate (Fig. 7c). The Damgad Formation (Fig. 7d), with a basal ~30 m thick conglomerate, rests in angular unconformity on top of the Melmura Formation (Gehrels et al., 2003). Lithologies in the Damgad Formation include fine- to medium-grained cross-stratified quartzite and occasional brown phyllite. However, Antolin et al. (2013) suggest that the TH rock in the klippe is bounded at the base by the STDS, rather than an unconformable contact.

Camping/lodging at Dadeldhura for the night (Camp 3 on Fig. 2).

DAY 4. Lesser Himalayan Duplex

The Ramgarh-Munsiari Thrust Sheet North of the Dadeldhura Klippe

North of the Dadeldhura klippe, the northern limb of the RMT sheet dips toward the south. At Arnakoli Khola, the Dumri Formation is sandstone and is cut by the RMT sheet (N29°24'8.6"; E80°37'24.7"; 2036±76 m). Based on this cross-cutting relationship and the minimum 15 Ma age of the Dumri Formation at Swat Khola, DeCelles et al. (2001) argued that the age of slip on the RMT must be younger than 15 Ma. Arnakoli Khola is ~130 km north of Swat Khola. Robinson & McQuarrie (2012) suggest that initial deposition of the Dumri Formation at Arnakoli

Khola was as early as 25 Ma, but it was cut by the RMT between 16 and 13 Ma.

In far-western Nepal, several previous workers mapped a “Bajang nappe,” another klippe of GH rocks north of the Dadeldhura klippe, near Hat village (Fig. 2; Bashyal, 1986; Amatya & Jnawali, 1996; Upreti & Le Fort, 1999). Our mapping in this region demonstrates the “Bajang nappe” does not exist; instead it is a klippe of the RMT sheet with the Proterozoic augen gneiss intruded into the Ranimata Formation.

The Lesser Himalayan Duplex

All of the LH rocks shown in Figure 5 are exposed in the Lesser Himalayan duplex. We previously discussed the Sangram, Syangia, and Ranimata formations. The rest of the LH rocks will be described as they are encountered along the route of the field trip. On the road to Patan, north of the exposure of Dumri Formation at Arnakoli Khola, is a sequence of tightly folded Sangram and Galyang Formations cropping out along the road (Fig. 8a). Before reaching the town of Patan, another road branches to the northeast that we will follow. The quality of this road depends upon the season. In the monsoon season, the road is frequently impassable.

Galyang Formation

The Galyang Formation consists of ~500-1,000 m of thinly bedded, strongly foliated, olive green, brown, and gray phyllite and black slate with occasional quartz augen. In far-western Nepal, the Galyang Formation contains an ~100 m thick interval of cherty, thinly bedded, siliceous dolostone termed Baitadi carbonates. Small-scale structures include folding and faulting. Although the Galyang Formation bears lithologic similarities with the Ranimata Formation and the Benighat Formation slates (see below), the Galyang Formation is thinner, less metamorphosed, and less chloritic than the Ranimata Formation. The upper contact of the Galyang Formation is not well exposed in western Nepal, but the same lithostratigraphic interval in central Nepal is transitional with the overlying Nourpul Formation, which is similar to the Syangia Formation of western Nepal (Upreti, 1996; DeCelles et al., 2001).

North of the alternating Galyang and Sangram

Formations, is a 50-100 km thick outcrop of the Syangia Formation at the village of Mili. The younger-on-older relationship suggests that the contact is a normal fault. The Syangia Formation has purple slate with raindrop imprints and desiccation cracks and transitions upward into the Lakhaparta Group.

Lakharpata Group

Three units compose the Lakharpata Group in far-western Nepal: a lower unit of blue-gray limestone and dolostones; a middle unit of black shale, limestone and dolostones; and an upper unit of blue-gray limestone and argillaceous dolostone. In central Nepal, these units have formal formation status (Sakai, 1985). The main rocks in the Lakhaparta Group carbonate units consist of laminated microcrystalline dolostone; thinly bedded, white quartzite (up to 100 m thick); and minor gray phyllite with occasional limestone beds. Stromatolites are abundant in both the upper and lower carbonate units. The middle black shale unit is probably equivalent to the Benighat Formation slates of central Nepal (Stöcklin, 1980; Sakai, 1985) and consists of black shale/slate, thin gray calcareous siltstone beds, gray phyllite, and black micritic beds. In far-western Nepal, the thickness of the Lakharpata Group is difficult to determine because it is intensely deformed. However, mapping suggests a thickness of ~3 km. The upper contact of the Lakharpata Group is a major unconformity with the overlying Gondwanan and/or Tertiary units.

This road travels along the ridge with deep valleys on either side of the road. North of the intensely deformed Lakharpata Group, the RMT crops out against the Benighat Formation (N29°32'13"; E80°46'40"). The road goes through the Ranimata Formation and the villages of Deulek (Figs. 8b, 8c). Camping near Deulek (Camp 4 on Fig. 2).

DAY 5. LESSER HIMALAYAN DU- PLEX

The road may end at the village of Sunkada (N29°30'17.9"; E80°51'23.2"; 1719±107 m) depending on the season, or the road may continue up the Seti River toward Chainpur. This field guide is written as if the traverse is made by hik-



Figure 7

(a) Dadeldhura Granite with a U-Pb age of 492 ± 6 Ma (DeCelles et al., 2001), finger for scale. (b) Photomicrograph of the Kalikot Schist of the Dadeldhura klippe, biotite (bi) and muscovite (ms) surrounding garnet (G) plus plagioclase (plag) and quartz (Q). Field of view is ~ 9 mm. (c) Melmura Formation, graphitic-carbonaceous rock along the Dadeldhura-Dipayal road with person at left for scale. (d) Damgad Formation, thin-bedded quartzite cropping out along the Dadeldhura-Dipayal with people for scale ($N29^{\circ}23'5.5''$; $E80^{\circ}37'12.7''$).

ing from Sunkada. At Sunkada, there is a stretch pebble conglomerate along the road in the Ranimata Formation. The road cuts through the RMT and the rock along the fault is white, sugary, and shattered quartzite (Fig. 8d). Also associated with the RMT is a cataclasite in the Lakharpata Group (Fig. 8e). The road/trail descends 1000 m from Sunkada down to the Kali Gad, passing through

exposures of the Lakharpata Group. Underneath the RMT, the stromatolitic Lakharpata carbonate rocks are intensely deformed (Figs. 8f, 9a, 9b) ($N29^{\circ}30'13.7''$; $E80^{\circ}53'05.8''$; 1027 ± 48 m).

Traverse south down the Kali Gad until the river intersects the Seti River at Deura. At Deura, a klippe of the RMT sheet is intersected again ($N29^{\circ}28'10.4''$; $E80^{\circ}53'47.5''$; 943 ± 147 m). If one

continues south on the Seti River, the entire RMT klippe is traverse and the Lakharparta Group crops out again on the south side of the klippe. However, to get to Chainpur, we will hike northeast up the Seti River. Hiking trails exist on both the south and north sides of the river. It is wise to consult the locals about whether the trail is open on the preferred south side. Northeast from Deura, you will hike out of the Ranimata Formation and cross the RMT into the Lakharparta Group (N29°27'37"; E80°57'05.8"; 850±150 m). On the south side of the Seti River, the RMT and Ranimata Formation are present up in the cliffs. At the village of Rail, the Syangia Formation crops out in the river as a dark, iron-rich quartzite even though the valley walls are composed of the Lakharparta Group.

Spend the night along the Seti River probably not near a village (Camp 5 on Fig. 2).

DAY 6. Lesser Himalayan Duplex

Last night's camp was in the Lakharparta Group, and the through the morning, you will be hiking through the deformed carbonate rock until just north of the Taru Gad. The intense deformation in the Lakharparta Group probably resulted from the superposition of the RMT hanging wall rocks, which have subsequently been eroded away. The RMT is exposed ~10 km south of the river as it dips southward underneath the Dadeldhura klippe. At the bridge across the Seti River to the Taru Gad, the stratigraphy transitions down section to the Syangia Formation (Fig. 9c). Stretched pebble conglomerates in the Syangia Formation (Fig. 9d) are present on both sides of the river. Along the Seti River, a small outcrop of green quartzite is interpreted as the Dumri Formation because of the presence of the Dumri Formation up the Taru Gad (Fig. 9e). A thrust exists between the Syangia and Dumri Formations. From the Dumri Formation, you will traverse down section into the Lakharparta Group. On the west side of the bridge at Malumela, there are overturned stromatolites (Fig. 9f) in the Lakharparta Group. Camping this night will be near the town of Malumela (N29°29'58.3; E81°06'22.7"; 1166±42 m) (Camp 6 on Fig. 2).

DAY 7. Lesser Himalayan Duplex

This section of the Seti River has the entire Lakharparta Group exposed. East of Malumela, you will encounter the Benighat Formation in a narrow gorge (Figs. 10a, 10b, 10c) (N29°30'12.8; E81°07'19.0"; 1195±116 m). After the black slates of the Benighat, the Lakharparta Group carbonates are again encountered (Fig. 10d) and deformation increases northeastward up the Seti River toward Chainpur. The amount of purple quartzite and green stretched pebble conglomerate float increases as the stratigraphy transitions down into the Syangia Formation marked by red and green shale (N29°31'00.2; E81°09'33.0"; 1157±46 m). After the Syangia Formation, you will hike into the Ranimata Formation. This is a thrust sheet in the northern part of the LH duplex; however, the boundary is complicated by structure and is now a normal fault (see Robinson et al., 2006 for a complete explanation and Figure 3b for the cross section). Hike to Chainpur in the Ranimata Formation.

Spend the night in Chainpur. Camping is possible in the school yard (Camp 7 on Fig. 2).

DAY 8. Chainpur to Talkot

Chainpur is located in the Ranimata Formation. However, within that formation there are significant quartzite interbeds. Figure 11a is a picture of folded quartzite beds located on the mountain on which Chainpur is built. Hiking northeast along the Seti River, you will pass out of the lower LH thrust sheet and into a window through the thrust sheet. In that window, you will see a hut along the trail with Syangia Formation slate purple roof tiles (Fig. 11b) and then on the west side of the river you will find laminated dolomite of the Baitadi carbonate rocks in the Galyang Formation (Fig. 11c) (N29°34'45.6"; E81°14'04.5"; 1310±150 m). The Bauli Gad is the river that flows into the Seti River from the north and there are exposures of the Gondwana sequence up this river (Fig. 11d). The Lesser Himalayan units described below are not in stratigraphic order but are arranged as they are encountered along the Seti River.

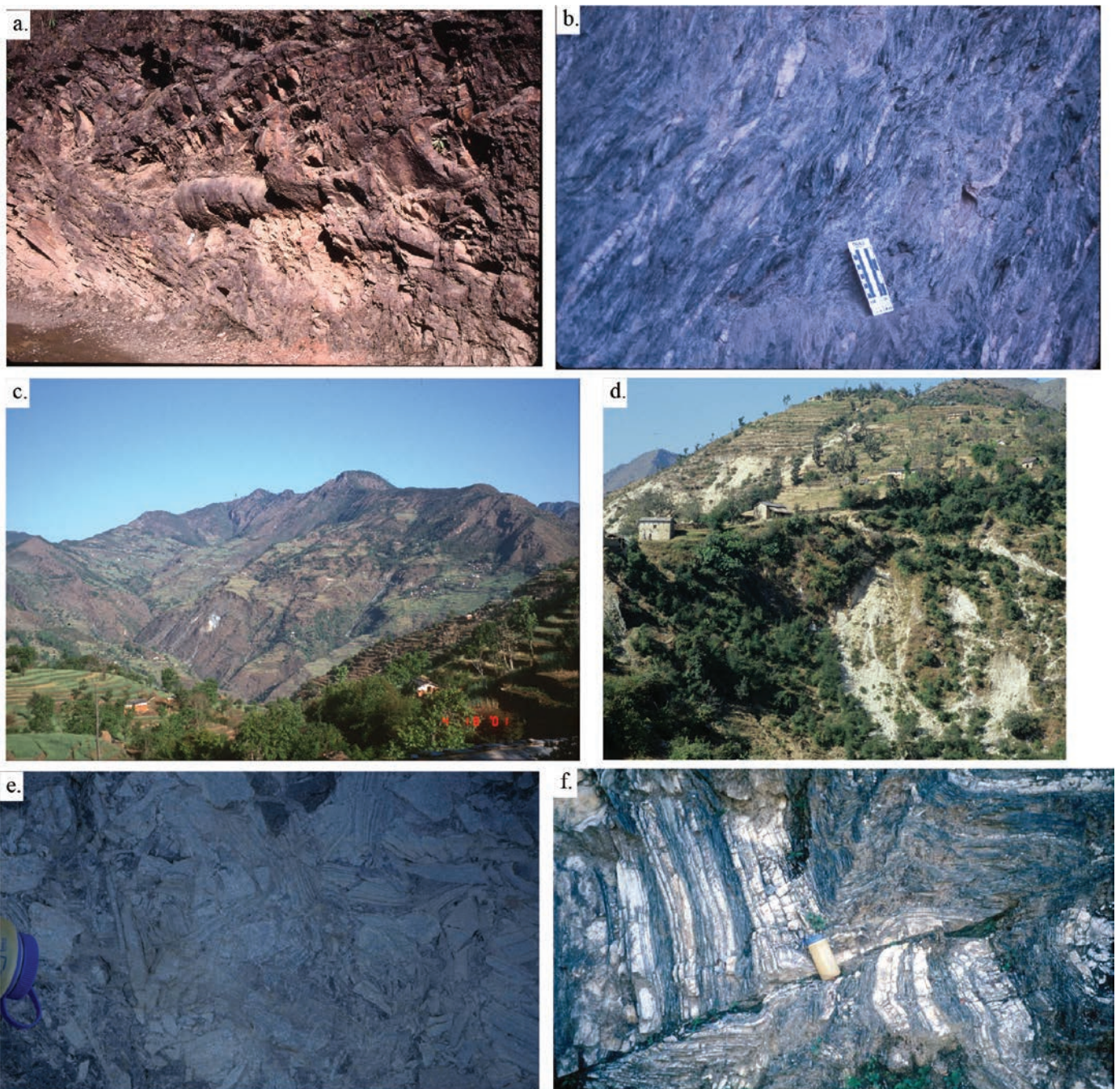


Figure 8

(a) Example of the meso-scale folds in the Galyang and Sangram formations along the Dadeldhura road, north of Dadeldhura (N29°24'27.6"; E80°37' 36.9"). (b) Ranimata Formation west of Deulek, showing typical quartz augen in sheared chloritic phyllite matrix. Long edge of scale is 20 cm. (c) Photo is from the village of Deulek looking west into the valley composed of the Ranimata Formation. (d) White schist just west of the village of Deulek. This photo is on the road and shows the shattered white rock that is common along the RMT in western Nepal (N29°32.261'; E80°48.524'; 7151±258'). (e) Cataclasite in the Lakharpata Group underneath the RMT near the Kali Gad (N29°35'59"; E80°54'23.7"; 1359±34 m), top of waterbottle for scale. (f) Deformation in the Lakharpata Group carbonate rocks underneath the RMT near the Kali Gad, north of Deura. One-liter waterbottle for scale (N29°31'47.5"; E80°43' 39.1").

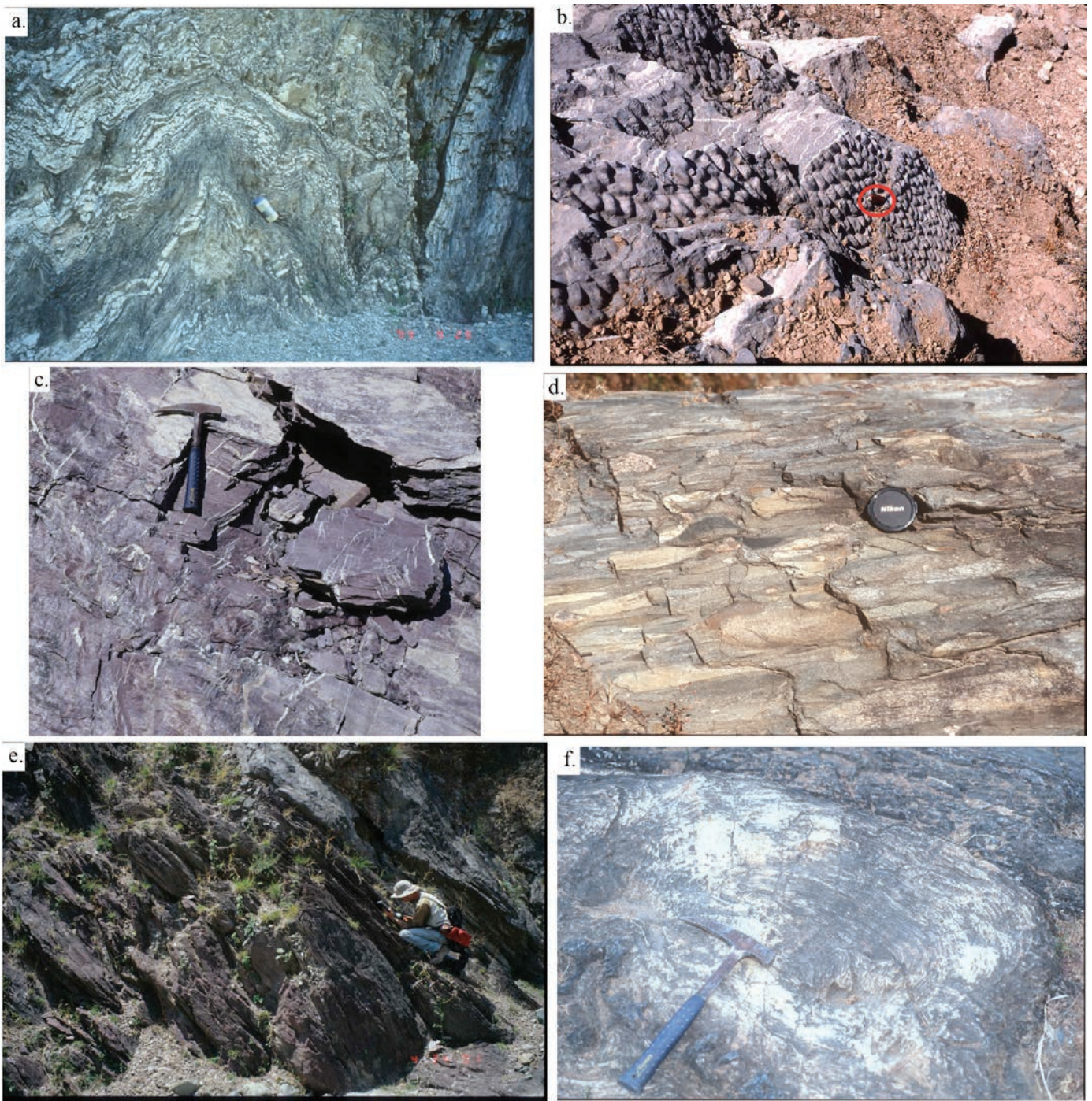


Figure 9

(a) Deformation in the Lakharpata Group carbonate rocks underneath the RMT near the Kali Gad, north of Deura. (b) Bedding plane view of stromatolites in the Lakharpata Group north of Deura. 5 cm red knife for scale has a red circle around it (N29°32'2.5"; E80°44' 8.5"). (c) Purple shale of the Syangia Formation with white quartz veins along the Seti River, 0.3 m rock hammer for scale (N29°29.543"; E81°04.637'; 3013±161'). (d) Syangia Formation stretched pebble conglomerate. Lens cap is 5 cm in diameter. (e) Dipping Dumri Formation red sandstone with a crouching Bob Gillis for scale (N29°30'08.5"; E81°03'40.2"). (f) Lakharpata Group stromatolites along the Seti River near the village of Malumela. Rock hammer is ~0.3 m long.

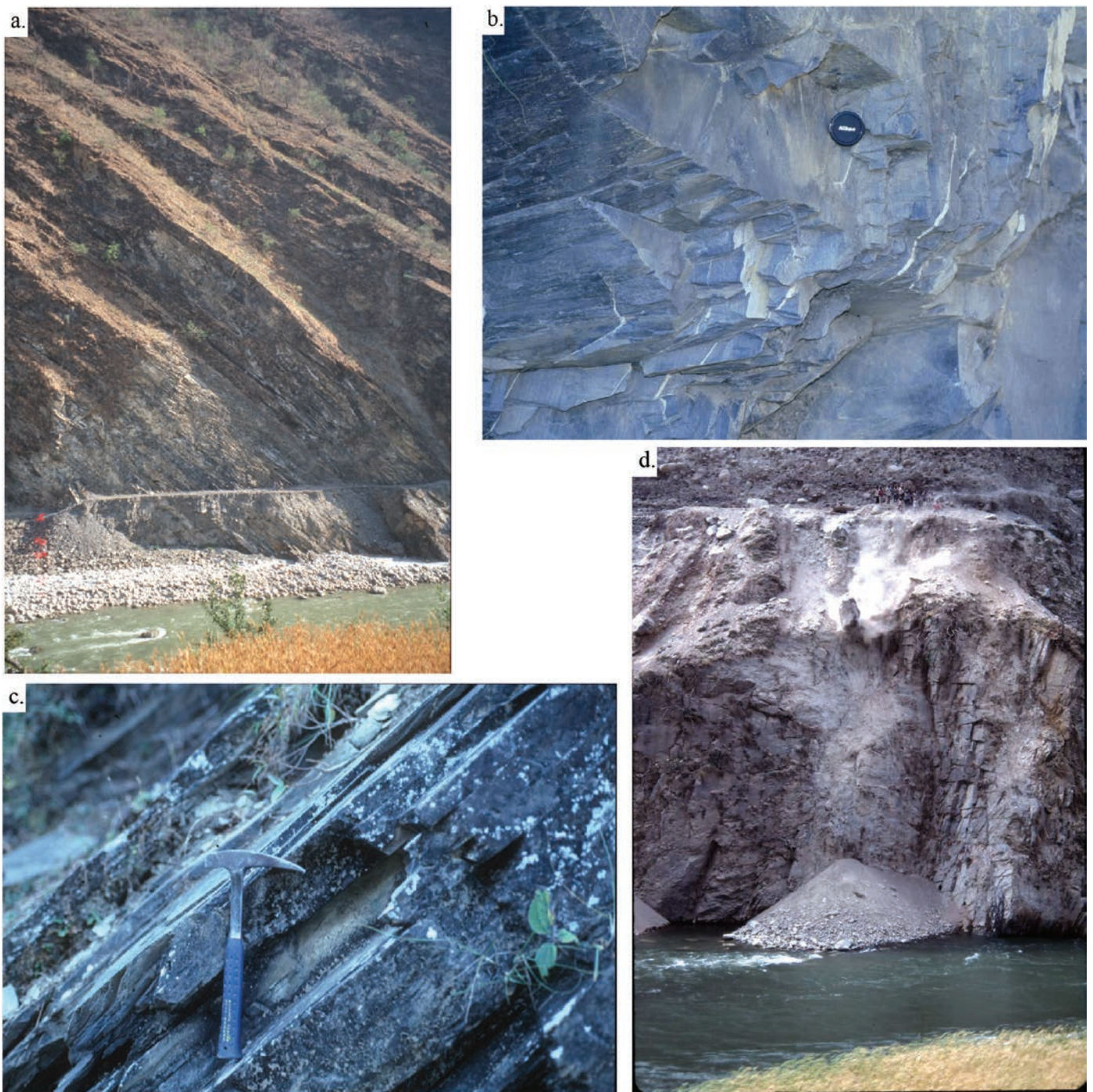


Figure 10

(a) Gorge in the Seti River composed of Benighat Slate in the middle of the Lakharpata Group (N29°34'45.6"; E80°14' 4.5"; 1310±150m). Trail by Seti River for scale. (b) Benighat Slate, 5 cm lens cap for scale. (c) Benighat Slate, 0.3 m rock hammer for scale. (d) Lakharparta Group south of Chainpur. Road workers dislodged the tumbling giant boulder that is plummeting toward the Seti River.

Gondwana Sequence

Resting unconformably on top of the Lakharpata Group in far-western Nepal is a several-hundred-meter thick succession of clastic sedimentary rocks of probable Late Cretaceous age that is readily assigned to the so-called Gondwana sequence. In central Nepal this succession also contains upper Carboniferous, Permian, and lower Mesozoic strata and have been studied in some detail by Sakai (1983, 1985, 1989). Additionally in central Nepal, the Gondwana sequence is an interval of quartzose sandstone, black shale, coal, lignite, and quartz pebble conglomerate. In far-western Nepal, the Gondwana sequence is poorly exposed. The main rocks consist of pebbly quartzose conglomerate and conglomeratic sandstone, black shale, and lignite.

Dumri Formation

Disconformably overlying the Bhainskati Formation is the lower Miocene Dumri Formation (Sakai, 1983; DeCelles et al., 1998b). Several kilometers north of Chainpur on the Bauli Gad and Suni Gad (Fig. 11e), a thick pebble conglomerate crops out in the Dumri Formation. The variegated cobble quartzite clasts and rosy quartz grains in the sandstone matrix suggest a semi-proximal location in Early Miocene time to the Himalayan thrust belt. It is possible that this conglomerate is older than the ~20 Ma at Chainpur. These outcrops north of Chainpur are the farthest north occurrences of this synorogenic sedimentary unit.

Continuing northeast along the trail along the Seti River east of Chainpur (Fig. 2), the lower half of the Dumri Formation is a green strongly indurated micaceous sandstone. At the base of the section, mottled purple and white bauxite paleosols (Fig. 11f) contain mainly kaolinite and hematite pisolites indicating a humid environment (N29°35'29.3"; E81°14'36.7"), similar to the paleosol that separates the Bhainskati and Dumri Formations at Dumri bridge. This disconformity is present along the entire Himalayan orogenic belt, and represents up to 15-20 myr of geologic time (DeCelles et al., 1998b). The upper half of the formation is dominated by red and green shale. Detrital white micas provide an $^{40}\text{Ar}/^{39}\text{Ar}$ age from the lower micaceous sandy section of ~20 Ma, which establishes the maximum age of the Dumri Formation in this location (DeCelles

et al., 2001; N29°35'14.0"; E81°14'36.7"; 1521±84 m). Further to the south near the MBT, Ojha et al. (2008) suggested an age of the Dumri Formation at Swat Khola of 19.9 to 15.1 Ma using magnetostratigraphy.

Dumri Formation lithologies include medium- to fine-grained, micaceous, quartzolitic sandstone; mottled siltstone; and pebble-cobble conglomerate, all of which are interpreted as fluvial deposits (Sakai, 1989; DeCelles et al., 1998b). The entire formation is >1200 m thick (DeCelles et al., 1998b). Conventional petrographic and U-Pb detrital zircon provenance data and Nd isotopic analyses indicate the Dumri Formation is a foreland basin deposit derived mainly from GH and LH rocks (DeCelles et al., 1998b; Robinson et al., 2001).

Detrital zircon U-Pb ages from the Dumri Formation (Table 1) reveal an age span similar to those of the Bhainskati Formation (e.g. ~500-800 Ma, ~1000-2100 Ma, ~2400-3200 Ma) except more grains are present in the 470-500 Ma and ~1000-1500 Ma age ranges (DeCelles et al., 2004). Because the detrital zircon age spectra for the GH and TH rocks are so similar (e.g. Amidon et al., 2005), they cannot be used to identify when GH rocks began to supply detritus. The average $\epsilon\text{Nd}(T)$ value is -14.4 for the Dumri Formation (Robinson et al., 2001) indicating that the formation is more isotopically evolved than Bhainskati Formation.

Within the Dumri Formation outcrop area, there are small exposures of the Bhainskati underneath the Dumri Formation. Within the window, there is a large-scale anticline with the axis trending at ~300°.

Bhainskati Formation

The oldest preserved synorogenic sediment from the growing Himalayan thrust belt is found in the middle to upper Eocene (Sakai, 1989) Bhainskati Formation (DeCelles et al., 1998b). In far-western Nepal, the Bhainskati Formation consists of ~100 m of black mudstone and thin beds of dark quartzose sandstone and fossiliferous limestone, and may be intensely deformed. This exposure of the Bhainskati Formation is rhythmically bedded black shale (Fig. 12a; N29°36'1.0"; E81°15'5.0").

Camping this night at Talkot (Camp 8 on Fig. 2).

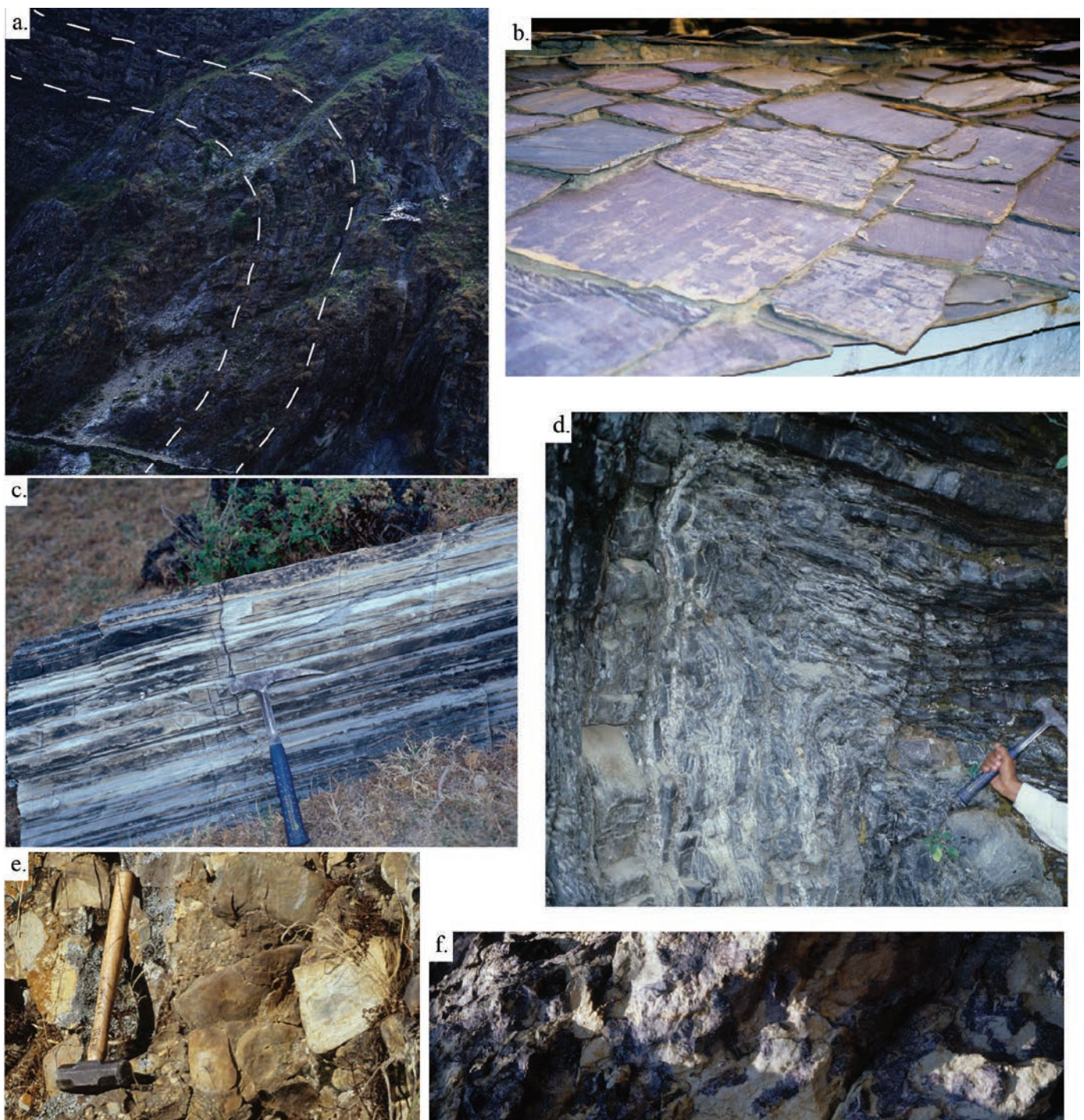


Figure 11

a) Fold in the Kushma Formation quartzite near Chainpur (N29°34'21.3"; E81°10' 24.5"; 4700'). Trail at the bottom of the picture for scale. (b) Purple slate of the Syangia Formation make for appropriate roof tiles, NE of Chainpur (N29°35.195"; E80°13.918'; 4747±492'). (c) Black and white banding in the Baitadi Carbonates of the Galyang Formation, northeast of the town of Chainpur. Rock hammer is 0.3 m long (N29°35'30.7"; E81°13' 42.9"; 5513±73'). (d) Interbedded black shale and quartzite in meso-scale fold in the Amile Formation of the Gondwana sequence. Om Pashad's arm and hammer for scale (N29°35.934'; E81°12.752'; 4795±240'). (e) Quartz pebble conglomerate with purple sandstone matrix in the Dumri Formation. Rock hammer for scale. Clasts are up to 10 cm in diameter (N29°35.811'; E81°13.197"; 5304±315'). (f) Dumri Formation Oxisols. Yellow patches are kaolinite and purple areas are hematitic. This is a paleolateritic soil. Hammer end for scale (N29°35' 29.3"; E81°14'36.7").

DAY 9. Northern Lesser Himalayan Duplex

On the northeast side of the fold in the window you will pass back into the Galyang Formation (Fig. 12b), which has been thrust southward on top of the Dumri and Bhainskati formations. At this location, the Galyang Formation slate has small-scale folds; similar structures are present in the underlying Dumri and Bhainskati formations. The last of the Galyang Formation exposures are just south of Talkot (N29°36'23.5"; E81°16'40.3"). From the Galyang Formation, you will cross another major thrust fault back into the Ranimata Formation (Fig. 12c). At Talkot, the trail and Seti River turn northward and the topography steepens (Fig. 12d). As you are traversing through this thrust sheet you will pass into a Proterozoic augen gneiss (Fig. 12e). Along the trail, exposures show that the contact between the Ranimata Formation and the augen gneiss is intrusive because there are veins of the augen gneiss intruded into the phyllite (N29°40'19.8"; E81°19'31.8" 2105±147 m).

Proterozoic Augen Gneiss

The augen gneiss is a medium-grained, foliated, L-S tectonite, and is present in Paleoproterozoic rocks across Nepal (LeFort, 1975; Pêcher & LeFort, 1977; Stöcklin, 1980; Phaplu augen gneiss of Maruo & Kizaki, 1981). Many workers have assumed that this augen gneiss is Indian basement and place a fault at the base of the gneiss (MCT-1; Arita, 1983). However, the Proterozoic augen gneiss intrudes the Ranimata Formation and yields a ca. 1.83 Ga U-Pb zircon age (DeCelles et al., 2000; Martin et al., 2011). Kohn et al. (2010) recalculated this age from DeCelles et al. (2000) to be 1.84±0.03 Ga. This age provides a minimum age boundary for the Ranimata Formation.

In far-western Nepal, thickness of the Proterozoic augen gneiss varies between 500 m and 10 km. Map patterns and foliations are concordant with those of the surrounding Ranimata Formation suggesting that the intrusions are sills. The edges of the intrusive bodies are mylonitic with top-to-the-south sense of shear indicators (Schelling, 1992), but internal parts of augen gneiss bodies are generally only slightly deformed. To the northeast of Chainpur, the Proterozoic augen gneiss is intruded by dioritic bodies.

Ramgarh-Munsiari thrust sheet and imbricates

Figure 12d is taken from the Proterozoic augen gneiss looking north up the Seti River. The ridges are supported by the quartzite carried on multiple thrust sheets in the LH duplex. The trail will descend along a side creek to the east and then ascend. As it ascends, the trail cuts through the Kushma Formation quartzite. In these exposures, there are garnets in hand sample, kyanite in thin section, and trough cross bedding in the outcrop. Balancing the cross section (Fig. 3b), helped to determine that the RMT doubles the thickness of the Kushma Formation in this location. The camping site is located at the base of the Kushma cliff near Ghat Khola (N29°43'14.7"; E81°20'49.1"; 2168±70 m). On the descent, you will pass into the Ranimata Formation.

Kushma Formation

Detrital zircons suggest that the Kushma Formation is ~1.85 Ga (DeCelles et al., 2000). The Kushma Formation is a structurally competent, medium- to coarse-grained, white to green ortho-quartzite with local muscovite-rich partings (Figs. 13a, 13b). Occasional quartz pebble conglomerate layers are present. Oscillatory current ripples, plane-parallel stratification, and planar and trough cross-stratification (Fig. 13b) are common sedimentary structures in the Kushma Formation. Mineral compositions include quartz + muscovite ± garnet ± kyanite. Generally, the Kushma Formation is thickly bedded and tabular, with zones of thinly bedded quartzite and green phyllite in its upper part. The Kushma Formation is 800–1000 m thick in far-western Nepal and crops out in high cliffs and rugged mountains (3-5 km elevation) south of the MCT. Meso-scale folds are usually absent except in the vicinity of major faults. The basal contact of the Kushma Formation is everywhere a thrust fault and the upper contact is transitional with the overlying Ranimata Formation. The Kushma Formation is strongly recrystallized near the MCT (Pearson, 2002) (Fig. 14e).

In far-western Nepal, the northernmost exposures of LH rocks in the LH duplex indicate peak temperatures of 500-550°C, based on Raman Spectroscopy of Carbonaceous Material (RSCM) (Bollinger et al., 2004). Beyssac et al. (2004) reported that the RSCM temperatures in LH rock along

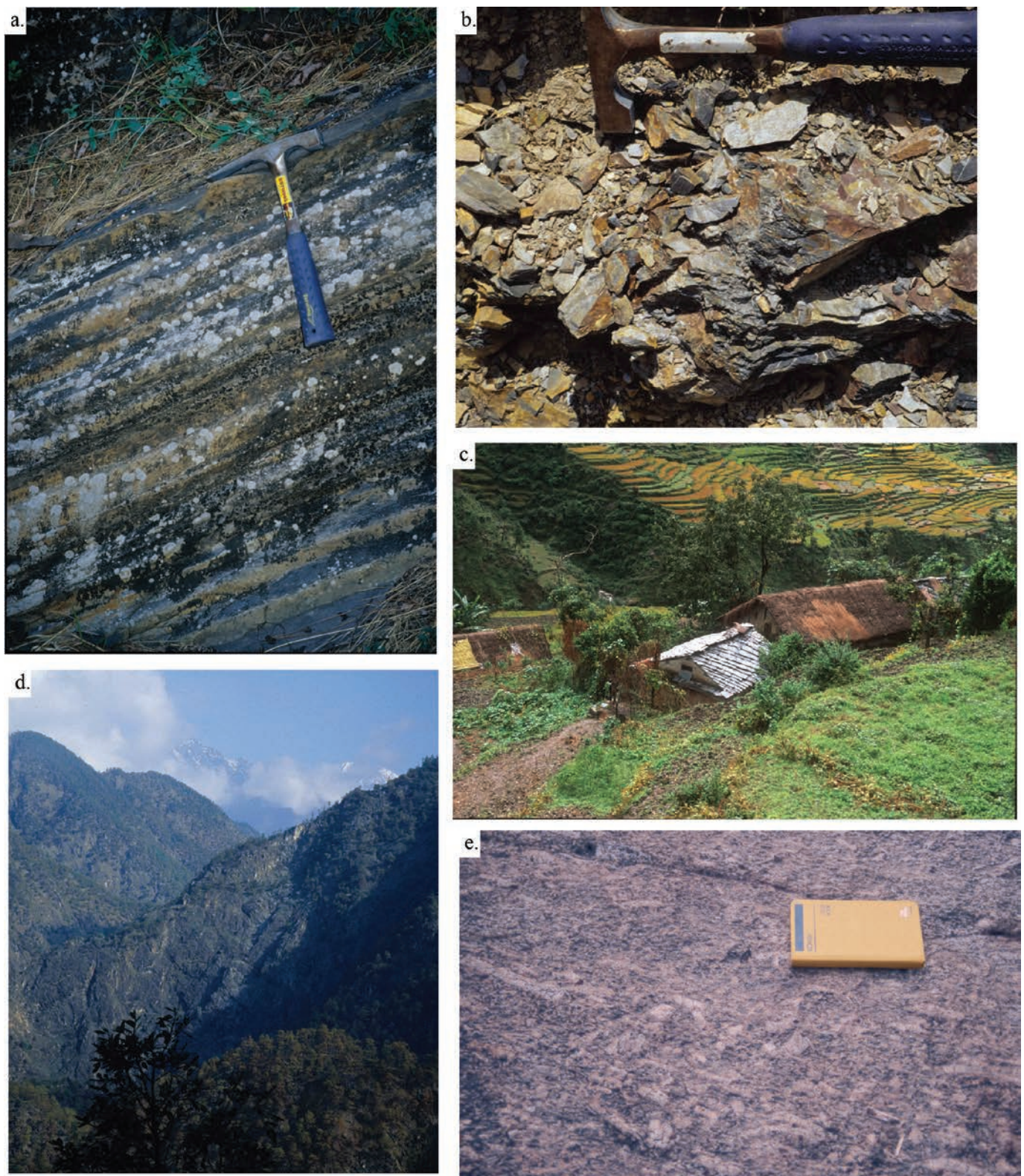


Figure 12

a) Bhanskati Formation of the Foreland Basin sequence. Black shale interbedded with light gray shale. 0.25 m hammer for scale (N29°35' 56.1"; E81°14' 52.4"; 1324±125 m). (b) Thin fissile brown phyllite of the Galyang Formation. 0.25 m hammer for scale (N29°36' 18.8"; E81°15' 59.6"; 4755±230'). (c) Roof tiles composed of the Ranimata Formation in the village of Talkot. (d) Photo is from the location in Figure 12e looking toward the north up the Seti River. Ridges of rock are in the Kushma Formation. (e) Proterozoic augen gneiss with S-C fabric. Field notebook is 15 cm long (N29°40' 19.8"; E81°19' 31.8"; 6907±492').

the Nepal/India border decrease gradually from 540°C in the footwall of the MCT to 330°C in the middle of the LH duplex. This southward decrease in temperature away from the MCT indicates that the magnitude of overburden that buried these samples also decreases southward. In addition, the RSCM data indicate that the northernmost LH rocks reached the temperatures necessary to reset $^{40}\text{Ar}/^{39}\text{Ar}$ muscovite ages. Robinson et al. (2006) reported an $^{40}\text{Ar}/^{39}\text{Ar}$ muscovite cooling age from the Ranimata Formation carried by the RMT sheet (SR123; N29°45'11.8; E81°16'6.6"; 2128 m) of 17-7 Ma (Table 2), and an $^{40}\text{Ar}/^{39}\text{Ar}$ muscovite cooling and isochron age of 12.5-12 Ma (SR103a) from the Ranimata Formation in the northern part of the LH duplex (Table 2).

Camping this night at Ghat Khola (Camp 9 on Fig. 2).

DAY 10. Northern Lesser Himalayan Duplex and Main Central Thrust

From Ghat Khola, return to the Seti River. Choose the lowest trail near the river because it has excellent exposures of the Ranimata Formation and mafic intrusions into the phyllite/schist, and the fault contact between Ranimata and Kushma formations, the RMT (Figs. 13 c-f; N29°45'33; E81°17'28.2"; 2125 m). On the way to the village of Dhuli, there are several repetitions of the Ranimata and Kushma Formations (Figs. 2, 3b). At Dhuli, the Ranimata Formation is a garnet-white mica-chlorite schist (Figs. 14 a-d)(SR103a; N29°46'29.2; E81°16'47.4"; 2534 m) with coarse-grained intrusive mafic rocks and rare carbonate interbeds. The Kushma Formation within the LH duplex horses has rare kyanite (Fig. 14f). To the north of Dhuli, the Ranimata Formation is more biotite- and garnet-rich, and the top-to-the-south sense of shear becomes more prominent (Fig. 15a).

Greater Himalayan rocks north of the Main Central thrust

Formerly, GH rocks have been regarded as Indian cratonic basement (e.g. Gansser, 1964; Mattauer, 1986; Srivastava & Mitra, 1994; Hauck et al., 1998). Several studies, however, show these rocks had Neoproterozoic and lower Paleozoic sedimentary protoliths and are nothing like cratonic India (Parrish & Hodges, 1996; Whittington et al., 1999; DeCelles et al., 2000; Ahmad et al., 2000; Robinson et al., 2001). Figure 15b is a picture of

the MCT in Ghat Khola separating LH from GH rocks. The contact between the two lithotectonic zones exhibits extreme shear strain (Figs. 15 c-d) and is located approximately 40 m north of N29°47'04.3"; E81°15'38.6"; 2554 m on the Seti River (Fig. 15e). Within the GH rocks are younger (15-20 Ma) leucogranite bodies that are decompression melts formed during exhumation of the GH rocks (Fig. 15f) (Harris & Massey, 1994; Visonà & Lombardo, 2002; Visonà et al., 2012).

In western Nepal, the GH rocks can be subdivided into three informal units (units I, II, and III; Fig. 2) first recognized in central Nepal (Le Fort, 1975; Le Fort, 1994; Colchen et al., 1986) (Figs. 16, 17). More specific descriptions of the GH rocks and shear zones are in Montomoli et al. (2013) and Carosi et al. (2010). Unit I consists of garnet- and kyanite-bearing pelitic gneiss, migmatite, and abundant metaquartzite with a middle- to upper-amphibolite facies metamorphic grade (Fig. 16a, 16c). The gneissic mineral assemblage includes quartz + biotite + muscovite + plagioclase + garnet ± kyanite ± cordierite ± epidote ± zircon (Figs. 17a, 17b). The metaquartzite contains quartz + muscovite + biotite ± plagioclase.

Within what we have mapped as unit I (~6 km thick) are thin (meters to tens of meters thick) lenticular bodies of diopside-, garnet-, phlogopite-, amphibole-bearing calcsilicate gneiss and marble (Fig. 16b). These thin bodies, if larger, would be mapped as unit II in other parts of Nepal. However, because these bodies are not mappable at the scale presented, we group them within unit I. Mineral assemblages in the calcsilicate gneiss (unit II) include calcite + quartz + potassium feldspar + plagioclase + hornblende + clinopyroxene ± sphene (Fig. 17c). Alternating layers of silicate minerals and calcite impart a "washboard" weathering habit to unit II (Fig. 16b).

Unit III contains mainly augen orthogneiss with a penetrative schistosity delineated by biotite and muscovite (beginning at N29°49'26.1"; E81°16'0.2"; 2652 m) (Fig. 16d). The mineral assemblage includes quartz + plagioclase + potassium feldspar + biotite + muscovite + garnet ± zircon ± apatite (SR 115) (Fig. 17d). Porphyroblastic feldspars are stretched and rotated with a top-to-the-south sense of shear. Similar orthogneiss bodies from other parts of the Himalaya yield Cambrian-Ordovician ages (e.g. Frank et al., 1977; Ferrara et al., 1983; Le Fort et al., 1983; LeFort, 1986; Pognante et al., 1990; Parrish & Hodges, 1996; Gehrels et al., 2003; 2006).

Camp this night is at the confluence of the Seti



Figure 13

a) Kushma Formation quartzite showing clean white quartzite beds, courtesy of Ofori Pearson. (b) Kushma Formation cross bedding, courtesy of Ofori Pearson. (c) Discovery of the RMT with joyous hand-waving Ofori Pearson for scale. (Figures 13c-f are at location N29°45'33.0; E81°17'28.2"; 6970'). (d) The RMT with Ofori Pearson for scale, location shown in Fig. 13c. (e) The Ranimata Formation in contact between the phyllite and mafic intrusives showing a chilled margin. Location shown in Fig. 13c. (f) The RMT at a different nearby outcrop showing the Kushma Formation quartzite in thrust contact with the footwall Ranimata Formation phyllite/schist.

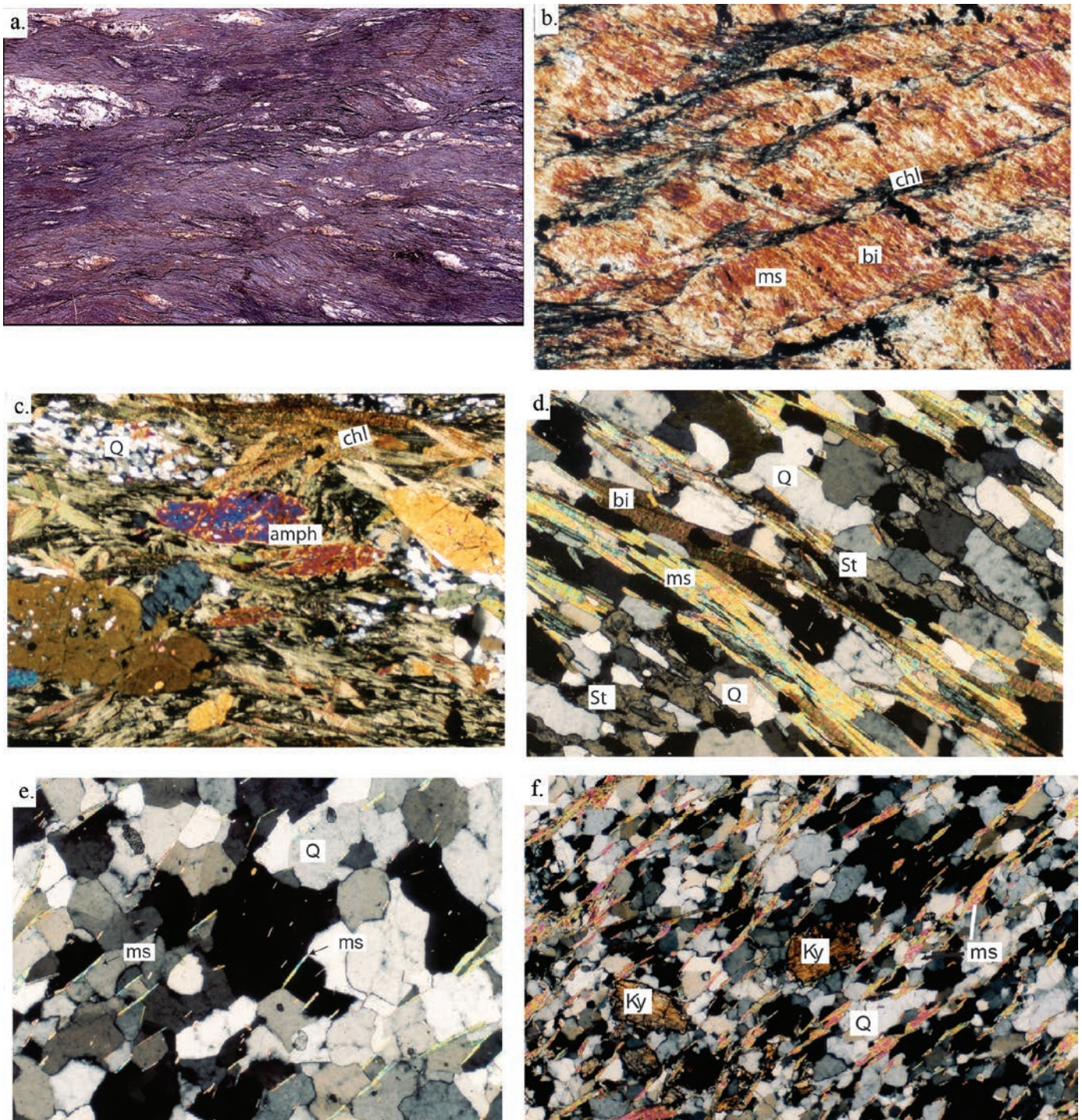


Figure 14

a) S-C fabric in the Ranimata Formation below the RMT south of Dhuli. (b) Crenulation cleavage in the Ranimata Formation; muscovite (ms), biotite (bi), chlorite (chl), quartz (Q). Field of view is ~4.5 mm. (c) Ranimata Formation mafic intrusive rock, containing amphibole (amph), chlorite (chl), and quartz (Q). (d) Staurolite (St) porphyroblasts in the Ranimata Formation. (e) Recrystallized coarse-grained quartzite in the Kushma Formation. (f) Strained fine-grained quartzite in the Kushma Formation with porphyroblasts of kyanite (Ky). Field of view for all photomicrographs is ~4.5 mm on the vertical.

Table 2
Hinterland Argon data.

Thrust Sheet	Reference	Sample	Figure	Age
DT/MCT, Budhiganga gneiss	DeCelles et al. (2001)	SR 40	4b	21.1±0.2 Ma
MCT, GH	Robinson et al. (2006)	SR 124	4b	ca. 25 Ma
DT/MCT, gneiss*	Sakai et al. (1999)	n/a†	n/a	25.68±0.13 Ma
RT, schist	Robinson et al. (2006)	SR 123	4c	17.8±0.8 to 7.3±0.5 Ma
Northern LH duplex, phyllite	Robinson et al. (2006)	SR 103a	4e	12.41±0.16 to 12.01±0.05 Ma

*Ar plateau age in biotite; All other ages are ⁴⁰Ar/³⁹Ar muscovite cooling ages

† n/a = not available

and Liyangwan Rivers (N29°49'55"; E81°15'15.3"; 2713±150 m) (Camp 10 on Fig. 2).

DAY 11. South Tibetan Detachment and TH rocks

Tibetan (Tethyan) Himalayan rocks north of the South Tibetan Detachment

At the confluence of the Seti and Liyangwan Rivers in far-western Nepal (Fig. 2), the South Tibetan Detachment (Fig. 18a) separates GH rocks from an ~2 km thick unit of impure marble and calcsilicate rocks that composes the TH basal unit (Figs. 18b, 18d; N29°51'29.6"; E81°12'39"; 3203±52 m). The South Tibetan Detachment runs parallel to the Seti River (Figs. 18c, 18e, 18f). The calcsilicate rocks and marble contain calcite + quartz + biotite + muscovite + clinozoisite + epidote + amphibole ± potassium feldspar ± plagioclase (Figs. 19e, 19f). Tabular and cross-cutting granitic leucosomes intrude the calcsilicate and marble. Small-scale ductile folds are abundant in the carbonate rocks (Fig. 18d), which in turn are cross-cut by steeply north-dipping brittle faults with a normal sense of displacement. In central Nepal, the base of the TH consists of the Sanctuary Formation, a dark gray siltite, slate, and quartzite interval. Above the Sanctuary Formation are massive marble and calcschist of the Annapurna Yellow and Nilgiri Formations, with a thickness of ~2–4 km and a probable Cambrian to Early Ordovician age (Colchen et al., 1986). The thick marble and calcsilicate units of far-western Nepal (Fig. 19b) may correspond to the Annapurna Yellow and Nilgiri Formations of central Nepal. Above the

calcsilicate rock is a pelitic schist intruded by a leucocratic granite (Fig. 19a; SR119). High camp is in a sheep grazing field within the pelitic schist (N29°52'19.4"; E81°10'16.1"; 3654±33 m) (Figs. 19b, 19c) along the Seti River.

Camping this night along the Seti River at the highest camp (Camp 11 on Fig. 2).

DAY 12. TH rocks

North of the basal TH rock unit, garnet-mica schist (quartz + biotite + muscovite ± garnet ± tourmaline) is banded with leucocratic granite for ~1 km (Fig. 19a). Northward, the garnet-mica schist is interbedded with pink and green coarse-grained quartzite with micaceous, calcsilicate, and phyllitic beds. This transition may be the Silurian to Cretaceous terrigenous and calcareous sediment of the upper part of the TH as seen in central Nepal (Colchen et al., 1986). The ability to hike northward from this camp is controlled by the condition of the trails and the amount of snow. Camp in the same location at high camp (Camp 12 on Fig. 2).

DAYS 13, 14 and 15. Return to Chainpur

On the first day, hike from the high camp to Ghat Khola (~8 hours) with no stops. The second day returning will be from Ghat Khola to Talkot or just south of Talkot. This is a very challenging hike and takes all day. The third day is from Talkot to Chainpur (Camps 13, 14 & 15 on Fig. 2).

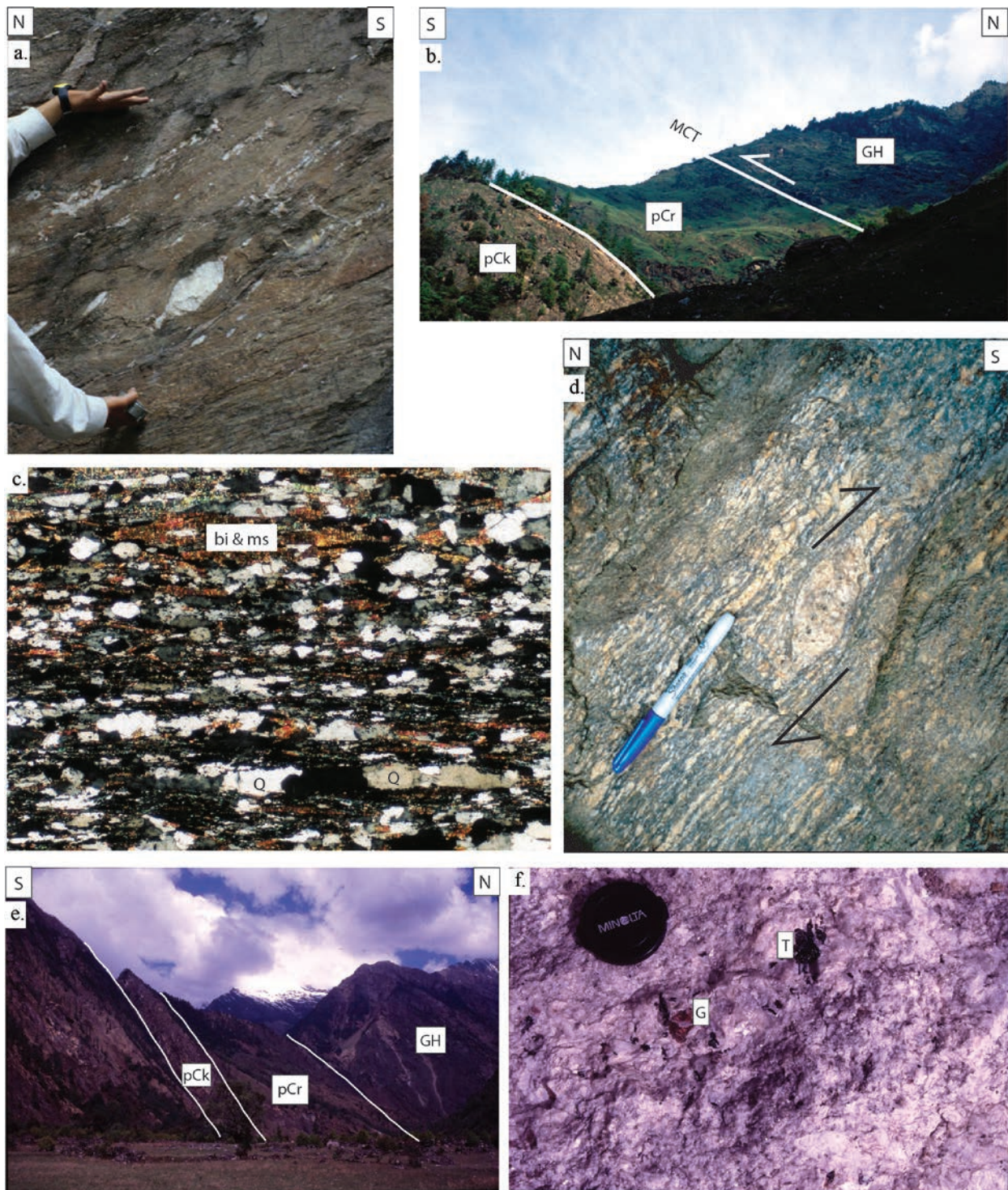


Figure 15

(a) Deformation in the LH Ranimata Formation in the immediate footwall of the MCT. Quartz auger shows a top to the south sense of shear ($N29^{\circ}47' 12.2''$; $E81^{\circ}15' 42.3''$; $8126 \pm 267'$). (b) The RMT sheet and the MCT along the Ghat Gad. The lower cliff is composed of Kushma Formation quartzite (pCk). The recessive rock above the quartzite is the Ranimata Formation (pCr). The MCT separates the Ranimata Formation from the resistant GH rocks above ($N29^{\circ}44' 50''$; $E81^{\circ}23' 10.4''$; $7453 \pm 129'$). (c) Photomicrograph of a highly strained rock in the "MCT zone". Mineral abbreviations are the same as those used in Figure 14. Field of view is ~ 4.5 mm on the vertical. (d) Rotation of a feldspar auger in unit III of the GH. The auger shows top-to-the-south sense of shear. Pen is ~ 8 cm long. (e) The position of the MCT across the Seti River toward the NW from the village of Dhuli. The fault zone is indicated by the white line separating pCr from GH. (f) Garnet and tourmaline-bearing two mica leucogranite, exposed north of Dhuli in the GH. (T) tourmaline, (G) garnet. Lense cap is 5 cm in diameter.

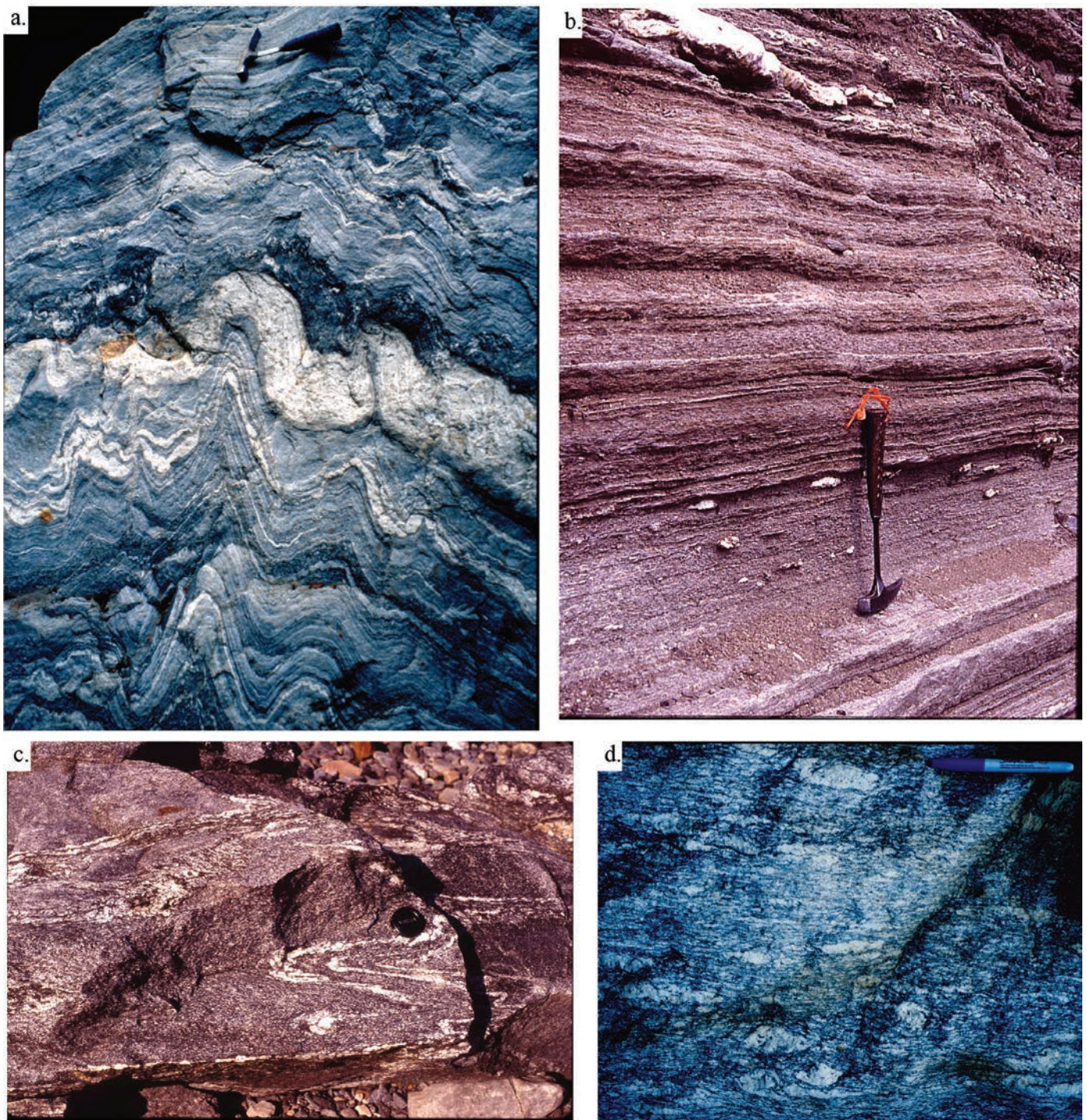


Figure 16

(a) Migmatitic banding in unit I of the GH. Rock hammer is 0.3 m long. (b) Strongly foliated calcite-pyroxene marble north of Dhuli in the GH unit 2. Rock hammer is 0.3 m long. (c) Migmatitic black biotitic gneiss, GH unit 1 north of Dhuli. Lens caps is 5 cm in diameter. (d) GH unit III augen gneiss.

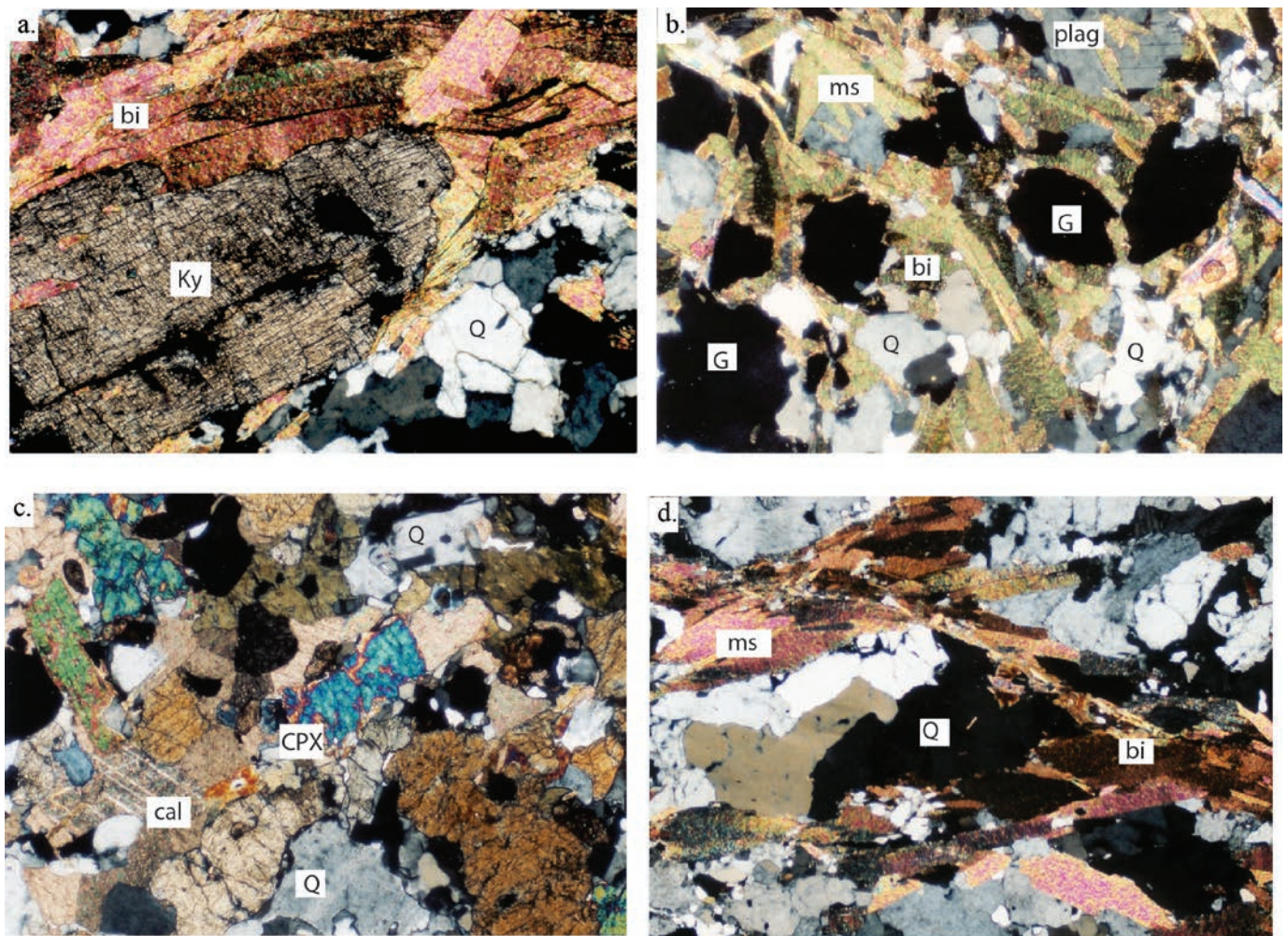


Figure 17

Photomicrographs of Greater Himalayan rocks north of Dhuli. (a) GH Unit I, large kyanite (Ky) crystal surrounded by biotite (bi), muscovite (ms) and quartz (Q). Field of view is ~4.5 mm. (b) GH Unit I, Garnet (G) porphyroblasts surrounded by biotite, plagioclase feldspar (plag). Field of view is ~4.5 mm. (c) GH Unit II, calcite (cal), clinopyroxene (CPX). Field of view is ~4.5 mm. (d): GH Unit II, schistosity is defined by the biotite and muscovite bands. Field of view is ~9 mm.

DAY 16. Return by airplane from Chainpur to Nepalgunj and Nepalgunj to Kathmandu

An alternative is to hike south from Chainpur to Dipayal for 4 days through Kaptad National Park and across the Dadeldhura klippe. At Dipayal, take the road west through TH rocks, join the Dadeldhura road and return south to Nepalgunj. This alternative route takes 5 days.

ACKNOWLEDGEMENTS

Robinson and DeCelles acknowledge the people of Nepal for their curiosity, their strong spirit, and

willingness to help with the hard work of long regional foot transects. The original field work was conducted from 1998-2001; this and several subsequent field seasons were supported by the National Science Foundation, and the Geological Society of America student research grants. Robinson was also supported through the University of Arizona's Department of Geosciences by the Mobil and Amoco Scholarship for student research, the GeoStructure Partnership grant, the Chevron Summer Research grant, and the ARCO Summer Scholarship for student research. Robinson and DeCelles thank Ofori Pearson, Senanu Pearson, Steve Ahlgren, Bob Gillis, Carmie Garzicone, Jay Quade, George Gehrels, Pete Kaminski, Brian Lareau, and Aaron Martin for their help in



Figure 18

a) The South Tibetan Detachment at confluence of the Seti and Liyangwan Rivers. The paragneiss (GH) is in the footwall and the calcsilicate rocks are in the hanging wall (TH). 0.3 m hammer is circled in red ($N29^{\circ}49'55''$; $E81^{\circ}15'51.2''$; $8900\pm 492'$). (b) Calcsilicate wall in the TH cross cut by leucogranitic dikes. Picture courtesy of Ofori Pearson. Pete DeCelles for scale. (c) The South Tibetan Detachment runs along the E-W flowing Seti River. Photo courtesy of Ofori Pearson. (d) Deformed cross cutting dikes in the TH. (e) Cliff trail in the TH with Ofori Pearson. GH is in the background south of the Seti River. (f) The trace of the STD runs along the valley with TH rocks on the left and GH rocks on the right. Rectangles indicate hanging wall of the fault.

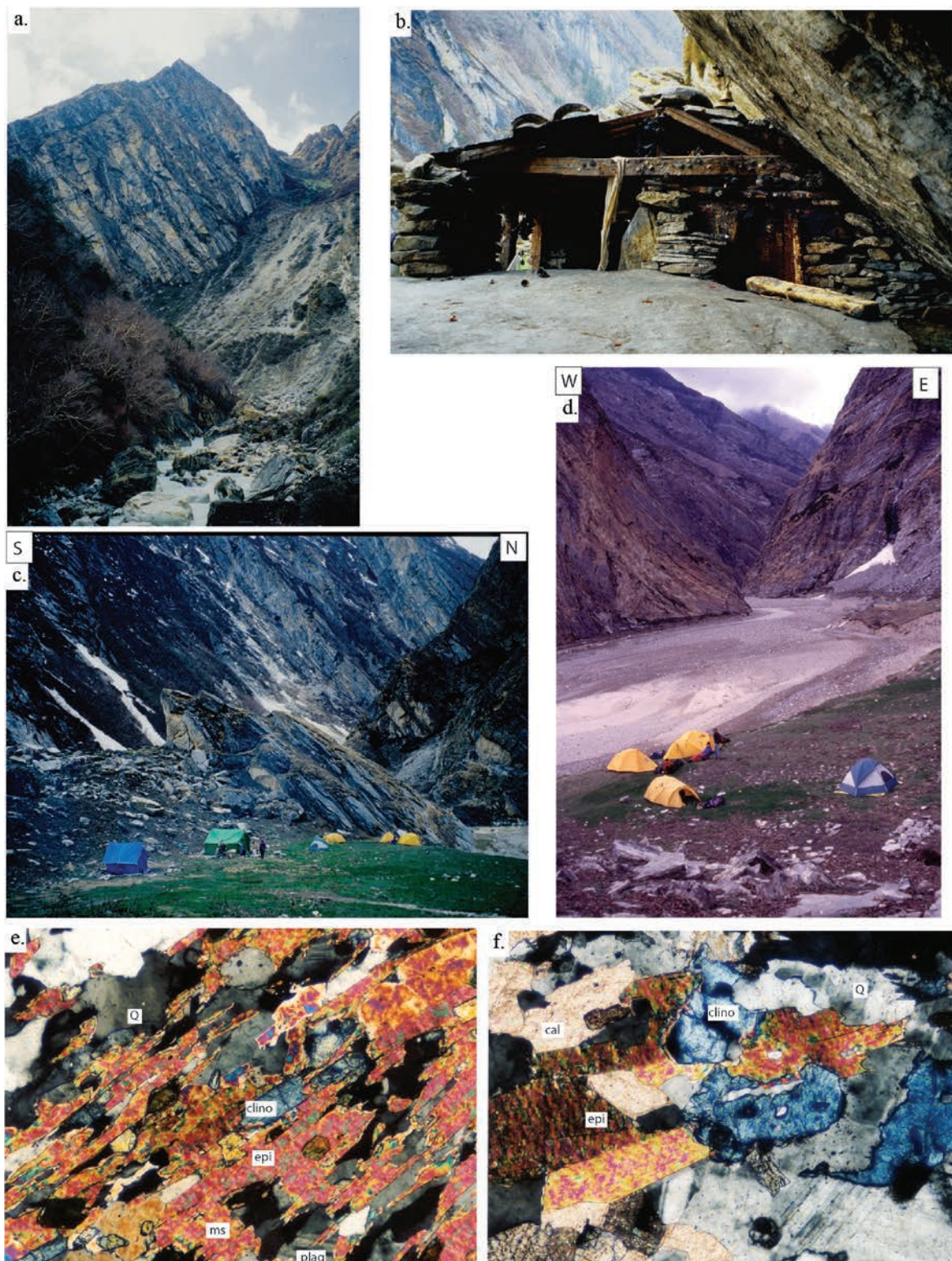


Figure 19

(a) Pelitic schist interbedded with leucocratic granite in TH. Cliff is several hundred meters high. (b) Shrine along the trail in the TH. Moderately north-dipping foliation in the Tethyan strata is visible at right. (c) Highcamp in the TH rock. View is toward the west ($N29^{\circ}52'19.4''$; $E81^{\circ}10'16.1''$; $11987 \pm 109'$). (d) Highcamp in the TH rock. View is toward the north up the canyon toward Tibet. (e) TH photomicrograph of calcsilicate rock shows clinozoisite (clino), epidote (epi), muscovite (ms), plagioclase (plag), quartz (Q). Field of view is ~ 2.2 mm. (f) TH photomicrograph. Rectangles indicate hanging wall of the fault.

the field and subsequent discussions. We thank Santaman Rai and editor Rudolfo Carosi for reviewing and improving this manuscript.

REFERENCES

- Ahmad, T., Harris, N., Bickle, M., Chapman, H., Bunbury, J., Prince, C., 2000, Isotopic constraints on the structural relationships between the Lesser Himalayan Series and the High Himalayan Crystalline Series, Garhwal Himalaya: Geological Society of America Bulletin, v. 112, p. 467-477.
- Amatya, K.M., and Jnawal, B.M., 1994, Geological Map of Nepal: scale 1:1,000,000, Royal Department of Mines and Geology, Kathmandu.
- Amidon, W.H., Burbank, D.W., and Gehrels, G.E., 2005, Construction of detrital mineral populations: insights from mixing of U/Pb zircon ages in Himalayan rivers: Basin Research, v. 17, p. 463-485, doi: 10.1111/j.1365-2117.2005.00279.x
- Antolin, B., Godin, L., Wemmer, K., and Nagy, C., 2013, Kinematics of the Dadeldhura klippe shear zone (W Nepal): implications for the foreland evolution of the Himalayan metamorphic core, Terra Nova, v. 25, p. 282-291, doi10.1111/ter.12034
- Appel, E., and Rösler, W., 1994, Magnetic polarity stratigraphy of the Neogene Surai Khola section (Siwaliks, SW Nepal), Himalayan Geology, v. 15, p. 63-68.
- Arita, K., Shiraushi, K., and Hayashai, D., 1984, Geology of western Nepal and a comparison with Kumaon, India: Faculty of Science Journal, Hokkaido University, Serial 4, v. 2, p. 1-20.
- Arita, K., 1983, origin of inverted metamorphism of the lower Himalaya, Central Himalaya: Tectonophysics, v. 95, p. 43-60.
- Bashyal, R.P., 1986, Geology of Lesser Himalaya, Far-western Nepal: Science de la Terre, Memoire 47, p. 31-42.
- Beyssac O., Bollinger L., Avouac J.P., and Goffé B., 2004, Thermal metamorphism in the Lesser Himalaya of Nepal determined from Raman spectroscopy of carbonaceous material: Earth and Planetary Science Letters, v. 225, p. 233-241.
- Bollinger, L., Avouac, J.P., Beyssac, O., Catlos, E.J., Harrison, T.M., Grove, M., Goffé, B., and Sapkota, S., 2004, Thermal structure and exhumation history of the Lesser Himalaya. Tectonics, v. 23, TC5015, doi:10.1029/2003TC001564.
- Carosi, R., Montomoli, C., Rubatto, D., and Visonà, D., 2010, Late Oligocene high-temperature shear zones in the core of the Higher Himalayan Crystallines (Lower Dolpo, Western Nepal). Tectonics, v. 29, TC4029. <http://dx.doi.org/10.1029/2008TC002400>.
- Colchen, M., LeFort, P., and Pêcher, A., 1986, Annapurna-Mansalu-Ganesh Himal: Paris, Centre National de la Recherche Scientifique, 136 p.
- DeCelles, P.G., Gehrels, G.E., Quade, J., Kapp, P.A., Ojha, T.P., and Upreti, B.N., 1998a, Neogene foreland basin deposits, erosional unroofing, and the kinematic history of the Himalayan fold-thrust belt, western Nepal: Geological Society of America Bulletin, v. 110, p. 2-21.
- DeCelles, P.G., Gehrels, G.E., Quade, J., and Ojha, T.P., 1998b, Eocene-early Miocene foreland basin development and the history of Himalayan thrusting, western and central Nepal: Tectonics, v. 17, p. 741-765.
- DeCelles, P.G., Gehrels, G.E., Quade, J., LaReau, B., and Spurlin, M., 2000, Tectonic implications of U-Pb zircon ages of the Himalayan orogenic belt in Nepal: Science, v. 288, p. 497-499.
- DeCelles, P.G., Robinson, D.M., Quade, J., Copeland, P., Upreti, B.N., Ojha, T.P., and Garzzone, C.N., 2001, Regional structure and stratigraphy of the Himalayan fold-thrust belt, farwestern Nepal: Tectonics, v. 20, p. 487-509.
- DeCelles, P.G., Robinson, D.M., and Zandt, G., 2002, Implications of shortening in the Himalayan fold-thrust belt for uplift of the Tibetan Plateau: Tectonics, v. 21, p. 1062-1087.
- DeCelles, P.G., Gehrels, G.E., Najman, Y., Martin, A.J., Carter, A., and Garzanti, E., 2004, Detrital geochronology and geochemistry of Cretaceous—Early Miocene strata of Nepal: Implications for timing and diachroneity of initial Himalayan orogenesis: Earth and Planetary Science Letters, v. 227, p. 313-330.
- Einfalt, H.C., Hoehndorf, A., and Kaphle, K.P., 1993, Radiometric age determination of the Dadeldhura granite, Lesser Himalaya, far-western Nepal: Schweiz. Mineral. Petrogr. Mitt., v. 73, p. 97-106.
- Ferrara, G., Lombardo, B., and Tonarini, S., 1983, Rb/Sr geochronology of granites and gneisses from the Mount Everest region, Nepal Himalaya: Geologische Rundschau, v. 72, p. 119-136.
- Frank, W., Thöni, M., and Purtscheller, F., 1977,

- Geology and petrography of Kulu-S. Lahul area: *Colloques Internationaux du Centre National de la Recherche Scientifique*, v. 268, p. 147-172.
- Fuchs, G., 1981, Geologic-tectonical map of the Himalaya: scale 1:2,000,000, Geological Survey of Austria.
- Gansser, A., 1964, *Geology of the Himalayas*: London, Wiley Interscience, 289 p.
- Gautam, P. and Rösler, W., 1999, Depositional chronology and fabric of Siwlaik group sediments in Central Nepal from magnetostratigraphy and magnetic anisotropy, *Journal of Asian Earth Science*, v. 17, p. 659-682.
- Gautam, P., Hosoi, A., Regmi, K.R., Khadka, D.R., and Fujiwara, Y., 2000, Magnetic minerals and magnetic properties of the Siwalik group sediments of the Karnali river section in Nepal, *Earth Planets Space*, v. 52, p. 337-682.
- Gehrels, G.E., DeCelles, P.G., Martin, A., Ojha, T.P., Pinhassi, G., and Upreti, B.N., 2003, Initiation of the Himalayan Orogen as an Early Paleozoic Thin-skinned Thrust Belt: *GSA Today*, v. 13, p. 4-9.
- Gehrels, G.E., DeCelles, P.G., Ojha, T.P., and Upreti, B.N., 2006, Geologic and U-Th-Pb geochronologic evidence for early Paleozoic tectonism in the Kathmandu thrust sheet, central Nepal Himalaya: *Geological Society of America Bulletin*, v. 118, p. 185-198.
- Gehrels, G., Kapp, P., DeCelles, P., Pullen, A., Blakey, R., Weislogel, A., Ding, L., Gynn, J., Martin, A., McQuarrie, N., and Yin, A., 2011, Detrital zircon geochronology of pre-Tertiary strata in the Tibetan-Himalayan orogen, *Tectonics*, v. 30, TC5016, doi:10.1029/2011TC002868.
- Harris, N., and Massey, J., 1994, Decompression and anatexis of Himalayan metapelites, *Tectonics*, v. 13, p. 1537-1546.
- Harrison, T.M., Copeland, P., Hall, S.A., Quade, J., Burner, S., Ojha, T.P., and Kidd, W.S.F., 1993, Isotopic preservation of Himalayan/Tibetan uplift, denudation, and climatic histories in two molasses deposits: *Journal of Geology*, v. 100, p. 157-173.
- Hauck, M.L., Nelson, K.D., Brown, L.D., Zhao, W., and Ross, A.R., 1998, Crustal structure of the Himalayan orogen at ~90° east longitude from Project INDEPTH deep reflection profiles: *Tectonics*, v. 17, p. 481-500.
- Huyghe, P., Galy, A., Mugnier, J.-L., and France-Lanord, C., 2001, Propagation of the thrust system and erosion in the Lesser Himalaya: geochemical and sedimentological evidence: *Geology*, v. 29, p. 1007-1010.
- Le Fort, P., 1975, Himalayas: The collided range, Present knowledge of the continental arc: *American Journal of Science*, v. 275-A, p. 1-44.
- Le Fort, P., 1986, Metamorphism and magmatism during the Himalayan collision, in Coward, M.P., Ries, A.C., eds., *Collision Tectonics: Geological Society of London Special Publication* 19, p. 159-172.
- Le Fort, P., 1994, French earth sciences research in the Himalaya regions: Kathmandu, Nepal, *Alliance Française*, 174 p.
- Le Fort, P., Debon, F., and Sonet, J., 1983, The lower Paleozoic "Lesser Himalayan" granitic belt: Emphasis on the Simchar pluton of central Nepal, in Shams, F.A., ed., *Granites of Himalayas, Karakorum and Hindu Kush*: Lahore, Pakistan, Punjab University, p. 235-255.
- Martin, A.J., Burgoyne, K.D., Kaufman, A.J., and Gehrels, G. E., 2011, Stratigraphic and tectonic implications of field and isotopic constraints on depositional ages of Proterozoic Lesser Himalayan rocks in central Nepal: *Precambrian Research*, v. 185, p. 1-17. doi: 10.1016/j.precamres.2010.11.003.
- Maruo, Y., and Kizaki, K., 1981, Structure and metamorphism in eastern Nepal, in Saklani, P.S., ed., *Metamorphic Tectonites of the Himalaya: Today and Tomorrow's Printers and Publishers*, New Delhi, p. 175-230.
- Mattauer, M., 1986, Intracontinental subduction, crust-mantle decollement and crustal-stacking wedge in the Himalayas and other collision belts, in Coward, M.P., Ries, A.C., eds., *Collision Tectonics: Geological Society of America Special Publication* 19, p. 37-50.
- Montomoli, C., Iaccarino, S., Carosi, R., Langone, A., Carosi, R., and Visonà, D., 2013, Tectonometamorphic discontinuities within the Greater Himalayan Sequence in Western Nepal (Central Himalaya): Insights on the exhumation of crystalline rocks: *Tectonophysics*, v. 608, p. 1349-1370. <http://dx.doi.org/10.1016/j.tecto.2013.06.006>.
- Mugnier, J. L., Huyghe, P., Leturmy, P., and Jouanne, F., 2004, Episodicity and rates of thrust sheet motion in the Himalaya (Western Nepal). In: *Thrust tectonics and hydrocarbon systems*, McClay, K.R., ed, *American Association of Petroleum Geologists Memoirs*, v. 82, p. 91-114. SPI Publisher Services, Ashland, VA, USA.
- Najman, Y., Johnson, C., White, N.M., and Oliver,

- G., 2004, Constraints on foreland basin and orogenic evolution from detrital mineral fission track analyses and sediment facies of the Himalayan foreland basin, NW India: *Basin Research*, v. 16, p. 1–24.
- Najman, Y., Bickle, M., Garzanti, E., Pringle, M., Barfod, D., Brozovic, N., Burbank, D., and Ando, S., 2009, Reconstructing the exhumation history of the Lesser Himalaya, NW India, from a multitechnique provenance study of the foreland basin Siwalik Group: *Tectonics*, v. 28, TC5018, doi: 10.1029/2009TC002506.
- Ojha, T.P., Butler, R.F., Quade, J., DeCelles, P.G., Richards, D., and Upreti, B.N., 2000, Magnetic polarity stratigraphy of the Neogene Siwalik Group at Khutia Khola, far western Nepal: *Geological Society of America Bulletin*, v. 112, p. 424-434.
- Ojha, T.P., Butler, R.F., DeCelles, P.G., and Quade, J., 2009, Magnetic polarity stratigraphy of the Neogene foreland basin deposits of Nepal: *Basin Research*, doi: 10.1111/j.1365-2117.2008.00374x.
- Parrish, R.R., and Hodges, K.V., 1996, Isotopic constraints on the age and provenance of the Lesser and Greater Himalayan sequences, Nepalese Himalaya: *Geological Society of America Bulletin*, v. 108, p. 904-911.
- Pearson, O. N., and DeCelles, P. G., 2005, Structural geology and regional tectonic significance of the Ramgarh thrust, Himalayan fold-thrust belt of Nepal: *Tectonics*, v. 24, TC4008, 10.1029/2003TC001617.
- Pearson, O.N., 2002, Structural evolution of the central Nepal fold-thrust belt and regional tectonic and structural significance of the Ramgarh thrust [Ph.D. thesis]: Tucson, University of Arizona, 230 p.
- Pêcher, A., and LeFort, P., 1977, Origin and significance of the Lesser Himalayan augen gneisses, in Jest, C., ed., *Ecologie et géologie de l'Himalaya: Science de la Terre*, v. 268, p. 319-329.
- Pognante, U., Castelli, D., Benna, P., Genovese, G., Oberli, F., Meir, M., and Tonarini, S., 1990, The crystalline units of the High Himalayas in the Lahul-Zaskar region (northwest India): Metamorphic-tectonic history and geochronology of the collided and imbricated Indian plate: *Geological Society [London] Special Publication* 74, p. 161-172.
- Ravikant, V., Wu, F-Y., and Ji, W-Q., 2011, U-Pb age and Hf isotopic constraints of detrital zircons from the Himalayan foreland Subathu sub-basin on the Tertiary palaeogeography of the Himalaya: *Earth and Planetary Science Letters*, v. 304, p. 356-368.
- Robinson, D.M., 2008, Forward modeling the kinematic sequence of the central Himalayan thrust belt, western Nepal: *Geosphere*, v. 4, p. 785-801, doi: 10.1130/GES00163.1
- Robinson, D. M., and O. N. Pearson (2013), Was Himalayan normal faulting triggered by initiation of the Ramgarh-Munsiari Thrust?, *Inter. J. Earth Sci.*, 102, 1773-1790, doi: 10.1007/s00531-013-0895-3.
- Robinson, D. M. and N. McQuarrie (2012), Pulsed deformation and variable slip rates within the central Himalayan thrust belt, *Lithosphere*, 4, 449-464, doi:10.1130/L204.1.
- Robinson, D.M., DeCelles, P.G., Patchett, P.J., and Garzzone, C.N., 2001, The kinematic history of the Nepalese Himalaya interpreted from Nd isotopes: *Earth and Planetary Science Letters*, v. 192, p. 507-521.
- Robinson, D.M., DeCelles, P.G., Garzzone, C.N., Pearson, O.N., Harrison, T.M., and Catlos, E.J., 2003, Kinematic model for the Main Central thrust in Nepal: *Geology*, v. 31, p. 359-362.
- Robinson, D.M., DeCelles, P.G., and Copeland, P., 2006, Tectonic evolution of the Himalayan thrust belt in western Nepal: Implications for channel flow models: *Geological Society of American Bulletin*, v. 118, p. 865-885; doi: 10.1130/B25911.1.
- Rösler, W., Metzler, W., and Appel, E., 1997, Neogene magnetic polarity stratigraphy of some fluvial Siwalik sections, Nepal, *Geophysics Journal International*, v. 130, p. 89-111.
- Sakai, H., 1983, *Geology of the Tansen Group of the Lesser Himalaya in Nepal: Memoire of Faculty of Science, Kyushu University, [D]*, v. 25, p. 27-74.
- Sakai, H., 1985, *Geology of the Kali Gandaki Supergroup of the Lesser Himalayas in Nepal: Memoirs of the Faculty of Science, Kyushu University, [D]*, v. 25, p. 337-397.
- Sakai, H., 1989, Rifting of the Gondwanaland and uplifting of the Himalayas recorded in Mesozoic and Tertiary fluvial sediments in the Nepal Himalayas in Taira, A., and Masuda, F., eds., *Sedimentary Facies in the Active Plate Margin: Terra Scientific Publishing Company, Tokyo*, p. 723-732.
- Schelling, D., 1992, The tectonostratigraphy and structure of the eastern Nepal Himalaya: *Tectonics*, v. 11, p. 925-943.

- Shrestha et al. 1987a, Geological map of far-western Nepal: scale 1:250,000, Royal Nepali Department of Mines and Geology, Kathmandu.
- Shrestha et al., 1987b, Geological map of mid-western Nepal: scale 1:250,000, Royal Nepali Department of Mines and Geology, Kathmandu.
- Stöcklin, J., 1980, Geology of Nepal and its regional frame: Geological Society [London] Journal, v. 137, p. 1-34.
- Srivastava, P., and Mitra, G., 1994, Thrust geometries and deep structure of the outer and lesser Himalaya, Kumaon and Garhwal (India): Implication for evolution of the Himalayan fold-and-thrust belt: Tectonics, v. 13, p. 89-109.
- Szulc, A.G., Najman, Y., Sinclair, H.D., Pringle, M., Bickle, M., Chapman, H., Garzanti, E., Ando, S., Huyghe, P., Mugnier, J.-L., Ojha, T., and DeCelles, P., 2006, Tectonic evolution of the Himalaya constrained by detrital ^{40}Ar - ^{39}Ar , Sm-Nd and petrographic data from the Siwalik foreland basin succession, SW Nepal: Basin Research, v. 18, p. 375-391, doi: 10.1111/j.1365-2117.2006.00307.x
- Tokuoka, T., Takayasu, K., Yoshida, M., and Hisatomi, K., 1986, The Churia (Siwalik) Group of the Arung Khola area, west central Nepal: Mem.Fac. Sci. Shimane Univ., v. 20, p. 135-210.
- Upreti, B.N., 1990, An Outline Geology of Far-western Nepal: Journal of Himalayan Geology, v. 1, p. 93-102.
- Upreti, B.N., 1996, Stratigraphy of the western Nepal Lesser Himalaya: a synthesis: Journal of Nepal Geological Society, v. 13, p. 11-28.
- Upreti, B.N., 1999, An overview of the stratigraphy and tectonics of the Nepal Himalaya: Journal of Asian Earth Science, v. 17, p. 577-606.
- Upreti, B.N., and LeFort, P., 1999, Lesser Himalayan crystalline nappes of Nepal: Problems of their origin, in Macfarlane, A., Sorhabi, R.B., and Quade, J., eds., Himalaya and Tibet: Mountain roots to Mountain Tops: Geological Society of America Special Paper 328, p. 225-238.
- van der Beek, P., Robert, X., Mugnier, J.-L., Bernier, M., Huyghe, P., and Labrin, E., 2006, Late-Miocene—Recent exhumation of the central Himalaya and recycling in the foreland basin assessed by apatite fission-track thermochronology of Siwalik sediments, Nepal: Basin Research, v.18, p. 413-434, doi: 10.1111/j.1365-2117.2006.00305.x
- Visonà, D., & Lombardo, B., 2002, Two-mica and tourmaline leucogranites from the Everest-Makalu region (Nepal-Tibet). Himalayan leucogranite genesis by isobaric heating?: Lithos, v. 62, p. 125-150.
- Visonà, D., Carosi, R., Montomoli, C., Tiepolo, M., and Peruzzo, L., 2012, Miocene andalusite leucogranite in central-east Himalaya (Everest-Masang Kang area): low-pressure melting during heating, Lithos, v. 144, p. 194-208.
- Whittington, A., Foster, G., Harris, N., Vance, D., and Ayers, M., 1999, Lithostratigraphic correlations in the western Himalaya—An isotopic approach: Geology, v. 27, p. 585-588.